

Copyright Warning & Restrictions

The copyright law of the United States (Title 17, United States Code) governs the making of photocopies or other reproductions of copyrighted material.

Under certain conditions specified in the law, libraries and archives are authorized to furnish a photocopy or other reproduction. One of these specified conditions is that the photocopy or reproduction is not to be “used for any purpose other than private study, scholarship, or research.” If a user makes a request for, or later uses, a photocopy or reproduction for purposes in excess of “fair use” that user may be liable for copyright infringement,

This institution reserves the right to refuse to accept a copying order if, in its judgment, fulfillment of the order would involve violation of copyright law.

Please Note: The author retains the copyright while the New Jersey Institute of Technology reserves the right to distribute this thesis or dissertation

Printing note: If you do not wish to print this page, then select “Pages from: first page # to: last page #” on the print dialog screen

The Van Houten library has removed some of the personal information and all signatures from the approval page and biographical sketches of theses and dissertations in order to protect the identity of NJIT graduates and faculty.

ABSTRACT

**EXPERIMENTAL STUDY
OF THE RISE OF A LARGE SPHERE
IN A VIBRATED BED OF MONODISPERSE SPHERES**

by
Loïc Vanel

As a simplified way to study size segregation mechanisms, the rise of a single large sphere in a vibrated bed of smaller monodisperse spheres is investigated. The time it takes for the ball to rise from the bottom of the bed to the surface is measured in a very wide range of vibration amplitude, frequency and acceleration. Rise regimes are identified and are classified according to the macroscopic behaviors displayed by the granular bed: heaping, convection without heaping and crystallization. The influence of the large sphere's size on the rise velocity is described. The scaling features of the vibration amplitude dimensioned by the diameter of the bed particles are presented.

A tracking technique has been used to follow the three-dimensional motion of the large sphere inside the bed. Trajectories corresponding to various vibrational states of the granular bed are described. Possible adaptations of the tracking technique are suggested.

**EXPERIMENTAL STUDY
OF THE RISE OF A LARGE SPHERE
IN A VIBRATED BED OF MONODISPERSE SPHERES**

by
Loïc Vanel

**A Thesis
Submitted to the Faculty of
New Jersey Institute of Technology
in Partial Fulfillment of the Requirements for the Degree of
Master of Science in Mechanical Engineering**

Department of Mechanical Engineering

January 1997

Blank Page

APPROVAL PAGE
EXPERIMENTAL STUDY
OF THE RISE OF A LARGE SPHERE
IN A VIBRATED BED OF MONODISPERSE SPHERES

Loïc Vanel

Dr. Anthony D. Rosato, Thesis Advisor Associate Professor of Mechanical Engineering, NJIT	Date
--	------

Dr. Rajesh N. Dave, Committee Member Associate Professor of Mechanical Engineering, NJIT	Date
---	------

Dr. Pushendra Singh, Committee Member Assistant Professor of Mechanical Engineering, NJIT	Date
--	------

BIOGRAPHICAL SKETCH

Author: Loïc Vanel
Degree: Master of Science
Date: January 1997

Undergraduate and Graduate Education:

- Master of Science in Mechanical Engineering
New Jersey Institute of Technology, Newark, NJ, 1996
- DEA de Physique des Liquides,
Université de Paris VI, Paris, France, 1995
- Maîtrise de Physique,
Université d'Orsay, Orsay, France, 1993
- Licence de Physique,
Université d'Orsay, Orsay, France, 1992

Major: Mechanical Engineering

Presentations and Publications:

E. Clement, L. Vanel, J. Rajchenbach, and J. Duran, "Pattern formation in a vibrated granular layer," *Phys. Rev. E* **53**, 2972 (1996).

L. Vanel, R. J. Dave, and A. D. Rosato, "Experimental observations of a rise of a single large sphere in a bed of granular material subjected to vertical vibration," World Congress of Chemical Engineering, San Diego, CA, July 1996.

L. Vanel, A. D. Rosato, and R. J. Dave, "Rise regimes of a large sphere in vibrated bulk solids," submitted to *Phys. Rev. Lett.* (1996).

This thesis is dedicated to

*my family
my friends
and especially
Linda*

ACKNOWLEDGMENT

I wish to express my gratitude to Dr Anthony D. Rosato for inviting me to work with him. I thank Dr Rajesh N. Dave for his support while Dr Anthony D. Rosato was in sabbatical year. I also thank Dr Pushpendra Singh for accepting to be a committee member.

I acknowledge Songyao Ren, Don Rosander, Joe Glaz and Dave Singh for their support during the course of this research.

I am grateful to the National Science Foundation and the Department of Energy for having funded this project.

TABLE OF CONTENTS

Chapter	Page
1 INTRODUCTION	1
1.1 General Overview	1
1.2 Segregation of Dry Granular Materials	2
1.3 Outline of Remaining Chapters	3
2 LITERATURE REVIEW	4
2.1 Early Work Describing Basic Properties	4
2.2 Phenomenology of a Vibrated Bed	5
2.3 Experimental Observation of Segregation in Vibrated Beds	8
2.4 The Contribution of Computer Simulations	11
2.5 Motivation	14
3 EXPERIMENTAL PROCEDURES	15
3.1 Objective of the Experiment	15
3.2 Description of the Experimental Setup	16
3.3 Experimental Parameters	17
3.4 Measurement Techniques	18
3.4.1 Tracking System	18
3.4.2 Use of a Simple Device: the Stopwatch	20
4 RESULTS : STUDY OF THE RISE TIME	21
4.1 Limitations	21
4.2 Rise Regimes	24
4.2.1 First Regime: Heaping and Convection	25
4.2.2 Second Regime: Convection in the Absence of Heaping	26
4.2.3 Third Regime: Crystallization	28
4.3 Scaling Properties of the Vibration Amplitude	32
4.4 More Observations on the Role Played by the Relative Acceleration	34
4.4.1 Rise Time at Fixed Frequency as a Function of Relative Acceleration	36

TABLE OF CONTENTS

(Continued)

Chapter	Page
4.4.2 Rise Time at Fixed Amplitude as a Function of Relative Acceleration . . .	37
4.4.3 “Inverse” Convection at High Relative Acceleration	37
5 RESULTS: TRACKING THE MOTION OF THE LARGE SPHERE	39
5.1 Phenomenology of Trajectories	39
5.2 Analysis of the Three-Dimensional Motion	51
5.3 Problems and Possible Improvements	61
6 CONCLUSION	64
REFERENCES	66

LIST OF FIGURES

Figure	Page
3.1 Granular bed surrounded by an antennae cage	19
4.1 Successive measurements of rise time for fixed vibration conditions	22
4.2 Correlations between temperature and rise time fluctuations	23
4.3 Dimensionless rise time Tf as a function of frequency f for several values of relative acceleration Γ	25
4.4 View of the top surface when the bed crystallizes	29
4.5 Dimensionless rise time Tf as a function of frequency f for several values of relative acceleration Γ	30
4.6 Average rise velocity as a function of size ratio Φ	31
4.7 Dimensionless rise time Tf as a function of dimensionless amplitude a/d for several values of relative acceleration Γ	33
4.8 Dimensionless rise time Tf as a function of dimensionless amplitude a/d for several values of vibration velocity $a\omega$	35
4.9 Dimensionless rise time Tf as a function of relative acceleration Γ for several values of amplitude a/d	36
5.1 Plot of the vertical position z as a function of time, in the case of heaping at large amplitude ($a/d=1.8$) and $f=7.5$ Hz.	40
5.2 Plot of the vertical position z as a function of time, in the case of heaping at small amplitude ($a/d=1.12$) and $f=12$ Hz.	41
5.3 Plot of the vertical position z as a function of time, in the case of convection without heaping at large amplitude ($a/d=1.8$) and $f=18$ Hz.	42
5.4 Plot of the vertical position z as a function of time, in the case of convection without heaping at small amplitude ($a/d=1.12$) and $f=18$ Hz.	43
5.5 Plot of the vertical position z as a function of time, in the case of inverse convection at large amplitude ($a/d=1.8$) and $f=27$ Hz.	45
5.6 Plot of the vertical position z as a function of time, in the case of inverse convection at small amplitude ($a/d=1.12$) and $f=27$ Hz.	46
5.7 "Whale" effect: Plot of the vertical position z as a function of time for $a/d=1$ and $f=25$ Hz.	47
5.8 "Whale" effect: Plot of the vertical position z as a function of time for $a/d=1$ and $f=30$ Hz.	48

LIST OF FIGURES
(Continued)

Figure	Page
5.9 Power spectrum corresponding to the trajectory of Fig. 5.5.	49
5.10 Power spectrum corresponding to the trajectory of Fig. 5.6.	50
5.11 Position of the large ball (r, θ, z) in a cylindrical coordinate system ($\mathbf{u}_r, \mathbf{u}_\theta, \mathbf{u}_z$). .	52
5.12 Plot of the vertical position z as a function of time for $a/d=1$ and $f=15$ Hz. .	53
5.13 Plot of the radial displacement r as a function of time for $a/d=1$ and $f=15$ Hz. .	54
5.14 Plot of the angular motion $Teta$ as a function of time for $a/d=1$ and $f=15$ Hz. .	55
5.15 Plot of the rotational motion $Alpha$ as a function of time for $a/d=1$ and $f=15$ Hz.	56
5.16 Plot of the rotational motion Psi as a function of time for $a/d=1$ and $f=15$ Hz.	57
5.17 Plot of the rotational motion Khi as a function of time for $a/d=1$ and $f=15$ Hz.	58
5.18 Plot of the vertical position z as a function of time for $a/d=1$ and $f=15$ Hz. The ball is initially touching the side walls..	59
5.19 Plot of the radial position r as a function of time for $a/d=1$ and $f=15$ Hz. The ball is initially touching the side walls..	60
5.20 Amplitude spectrum for $a/d=1.8$ and $f=27$ Hz showing a high frequency peak whose origin is undetermined.	62

CHAPTER 1

INTRODUCTION

1.1 General Overview

The term granular material refers to a mixture made up of discrete solid particles. In nature, some examples are sand, pebbles, heaps of rock, heaps of earth, sediments or granular snow. The processing of natural resources, ore extraction and harvesting of cereals, vegetables and fruits produce huge quantities of granular material. Flour, sugar, salt are commonly found in a kitchen ! The industry is also a big producer of synthesized products, such as pharmaceutical powders or plastic grains.

Geophysical and environmental considerations are worth noting. There are undesirable natural disasters such as mud slides and rock or snow avalanches. Some ecological problems involve deposition of waste in water or pollution clouds. Even earthquakes involve dynamics of rocks which are submitted to very high stresses and suddenly break apart. At a much larger scale, asteroids' belts in the solar system liberate pieces into space which may impact the Earth.

In industry, granular materials are used in almost any field. Common technical problems are related to manufacturing, handling and processing in areas such as pharmaceutical, foodstuffs, detergent and chemical industries as well as high tech processing of ceramics and powder metal forming. Granular materials are used mainly in mixing, segregation, storage, flow, gas fluidization, conveying, size enlargement and size reduction operations. Despite the ubiquity of granular materials, the understanding of their behavior is so poor that fundamental research became a crucial economical issue for industry. Since engineers started to extensively investigate this field, more than forty years ago, progresses have been slow. The efficiency of recently built factories is still far off the predictions made by available models. Too often, scale-up of small model tests to the full scale industrial prototype is fraught with uncertainty. Engineers are reduced to trial and error methods, usually simple, but expensive in time and money. Obviously, granular materials present enormous difficulties to master because the knowledge of these materials remains elusive.

In recent years, the body of theoretical work has been increasing very fast, in part due to the new interest of the physics community in this field. A distinction has been made between dry and wet granular materials. Dry granular materials display double-faced behavior, either similar to a solid or a fluid. When at rest, they form heaps but if perturbed, they begin to flow. Wet granular materials are called slurries or suspensions and their behavior is strongly dependent on the fluid characteristics. Available theoretical tools generally fail to properly describe the behavior of dry or wet granular materials. In the case of dry granular materials, one could think it is sufficient to use mechanics concepts since the laws of solid dynamics are well established. However, the resolution of Newtonian equations for a system with a large number of bodies becomes mathematically unfeasible. Statistical theory is also not directly applicable, because there is no equivalence with the concept of temperature and because there is dissipation of energy by collisions and friction between the particles. Some important efforts have been made to develop adapted kinetic theories [1-2-3] but there are not enough experimental results to determine the relevance of these theories. Computer simulations are also a powerful tool. Though they can not replace experiments, they provide some interesting insights and allow the testing of old and new models. In the case of wet granular materials, parts of the phenomenon are explained through the use of fluid dynamics equations, especially when the concentration of particles is very low, but at high concentrations granular interactions become dominant and difficulties show up again. The study of dry granular materials is usually carried with the hope that the gas effects are avoided. Most important is the fact that a granular material is a highly non-linear and dissipative medium, which possesses characteristic features commonly found in non-linear dynamical systems.

1.2 Segregation of Dry Granular Materials

The term segregation refers primarily to the unmixing of an originally homogeneous granular mixture. This can happen whenever the granular material is made to move. Important efforts have been made to understand this usually unwelcome effect in the industrial processing of granular materials (see Ref [4] and [5] for a review on mixing problems). Segregation is typically observed when pouring a heap, and when stirring,

shearing or vibrating a mixture [6]. It appears that discrepancy in sizes is the most important cause of segregation. Segregation is often explained as the result of the “percolation” of small particles through the spaces between larger particles. When vibration is used, segregation has been described as the consequence of a convective flow and a trapping mechanism of the larger balls on the bed surface. Other mechanisms involving geometrical considerations, local reorganizations of the bed structure and/or collective effects such as arching or bridges have also been proposed.

In this thesis, we propose a study of the rise of a large ball placed at the bottom of a vibrated bed, which is a simple example of size segregation process. The starting point of our study is to describe the evolution of the rise time with the vibration parameters and the possible connections with other commonly observed phenomenon in vibrated beds such as heaping, surface waves, subharmonic instabilities, convection and compaction. The hope is to be able to identify more clearly the conditions for segregation. Besides the measurements of rise time, it is possible to obtain the full three-dimensional trajectory of the large ball during its rise. This can be done with the use of an advanced tracking technique developed at the Particle Technology Center, which is based on magnetic induction and involves electronics and software. The knowledge of the ball trajectory is likely to give additional understanding of segregation.

1.3 Outline of Remaining Chapters

Chapter 2 is a detailed literature survey on the phenomenology of vibrated beds, with a focus on segregation problems, for which both experimental and computer simulations’ results are presented. Chapter 3 describes the experimental setup and explains the two types of investigations carried : the measurements of rise time and the recording of rise trajectories. The results are presented in Chapter 4 for the rise time measurements and Chapter 5 for the description of trajectories. Chapter 6 discusses briefly the results before the concluding remarks.

CHAPTER 2

LITERATURE REVIEW

The following literature review is mainly restricted to the study of dry granular materials. Basic experiments are described and some simulations closely related to our work are presented. A large place is given to systems submitted to vibrations because it is relevant to the subject of this thesis and very rich in phenomena.

2.1 Early Works Describing Basic Properties

Some of the earliest studies of granular flows were performed by two fluid mechanicians, G. Hagen and O. Reynolds. In 1852, Hagen [7] performed experiments which showed that for granular flow, the flow rate through an orifice is independent of h , the head of material above the orifice, in contrast with the flow of a fluid where it depends upon \sqrt{h} . In 1885, Reynolds [8] introduced the idea of *dilatancy* which he defined as the property possessed by a granular media to alter its volume in accordance with a change in arrangement of its grains. To illustrate the phenomenon of dilatancy, Reynolds put together an apparatus consisting of a rubber bag filled with a mixture of granular material and water which was purged of any bubbles and then tied to a glass tube. When the bag is squeezed, one's naive intuition suggests that the water level in the tube would rise. But, instead, it goes down. What happens is that when squeezing the bag by hand, it is not possible to apply uniform pressure all around the outside and shear deformations develop. From geometrical considerations the bulk has to expand and water rushes in to fill the void spaces created. In the initial state the spherical grains are closely packed, then when the bulk is sheared, particle riding over each other and a vertical expansion occurs. Reynolds used these ideas about dilatancy to explain a phenomenon which can be observed when walking along the seashore. When one's foot is planted on the moist sand, shear and dilatation occur and the area around the foot immediately becomes dry. But, when the foot is raised, water is drawn in to occupy the additional voids created, and a pool of water soon collects in the footprint.

2.2 Phenomenology of a Vibrated Bed

In this section, we give an overview of the various behaviors observed in a vibrated bed of mainly monodisperse (uniform size) spheres.

The behavior of a vibrated granular bed is conditioned by the existence of two opposite energetic fluxes. The vibration acts as an energy reservoir while the collisions and frictional contact between the particles dissipate energy. Generally, a steady state arises in a system when the input and output energy flux become equal. The phenomenology of granular behavior is thus strongly dependent on the vibration parameters and on the dissipative properties of the particles, the container and sometimes the ambient gas.

Besides the vibration amplitude a and frequency f , a parameter used frequently is the relative acceleration $\Gamma = a\omega^2/g$, where $\omega = 2\pi f$ and g is the gravity. The relative acceleration is a parameter which arises naturally in the description of the motion of a particle on a loud-speaker. A particle initially at rest will separate from the loud-speaker plate only if $\Gamma > 1$, i.e. if the plate acceleration can become bigger than gravity. The particle starts a free flight when the plate acceleration is equal to gravity, and later collides again with the plate. It can be shown that the larger is the relative acceleration, the longer is the flight time in unit of vibration cycle, or the larger is the launch velocity in unit of maximum plate velocity. For low acceleration, the motion of a completely inelastic ball has simply the vibration periodicity T , but as acceleration is increased, a cascade of flight time bifurcations starts, leading to a $2T$, $4T$, $8T$... periodicity, until the flight time becomes again single valued and the motion periodicity $2T$. When the acceleration is further increased, similar scenario of flight time bifurcations are observed, ending successively by a $3T$, $4T$, $5T$... periodic motion. When a granular bed is slightly vibrated, there is no relative motion between the particles and the bed behaves as a solid. Furthermore, due to the multiple collisions occurring in a dense packing of inelastic grains, granular agitation can be quickly damped for small enough vibrations and the bed will behave as a single inelastic body. In a first approach, the relative acceleration has been used to characterize the bed behavior, even in the cases where the behavior is much more complex than the motion of one single particle.

In 1831, Faraday [9] observed that vibrated powder forms a heap generated by a convective motion : “...the particles of the heap rise up at the centre, overflow, fall down upon all sides, and disappear at the bottom, apparently proceeding inwards”. Much later, because of many potential applications in chemical engineering, this phenomenon has been studied in various geometries and with different types of periodic excitations by Kroll [10] in 1955, Rátkai [11] in 1976, or Savage [12] in 1988. All the fundamental studies enumerated now concern vertical sinusoidal vibration of a flat floor. In 1989, Evesque et al [13] established experimentally that the relative acceleration is the threshold parameter of convection. Laroche et al [14] showed that convection was a result of the interaction between the granular and the surrounding gas, but Pak et al [15] found that the gas effect occurs only for small particles. For larger particles, Clément et al [16] observed the formation of a heap (referred as heaping) driven by small convective rolls generated at the container walls due to frictional contacts, with the additional condition that the particles inelasticity and friction is sufficiently high. Rajchenbach [17] proposed a model based on the Reynolds’ concept of dilatancy [5] and described the existence of an internal flux of matter from more agitated to less agitated regions. Knight et al [18] studied convection as a segregation mechanism (see also 1.2.4), and gave recently a precise description of the flow field [19].

In the literature, fluidization is a term which most often refers to the granular agitation induced by an upward high velocity gas flow. By analogy, in vibrated bed, fluidization refers to the agitation of grains due to collisions with the vibrating plate. Kinetic theories [20] have predicted that kinetic energy, and thus fluidization, is bigger at the bottom of the bed where is the vibrating plate, i.e. the source of energy. In contrast, the experiments of Evesque et al [21] showed that fluidization is confined in the upper layers of the material. In a study of surface fluidization, Clément [22] observed that the top particles reach a state of random agitation, while the lower part of the bed remains compact. The bed structure was observed to be independent of the vibration phase, but not the internal agitation of grains. When the vibration is strong enough for the whole bed to be fluidized, Warr et al [23] found a velocity distribution close to a Boltzmann

distribution and measured a granular temperature following a power law dependency on the maximum velocity of vibration.

Wave-like patterns are commonly observed in vibrated granular materials. Douady et al [24] described a subharmonic instability where dense regions of particles oscillate out of phase, creating a pattern of periodic arches. This is due to the coexistence of two solutions (degenerated solutions), each of which has a periodicity double that of the vibration period. Note this is different from period-doubling where there is alternance between two solutions, from one period of vibration to the other. Pak et al [25] observed a wave traveling up the slope of a heap. Clément et al [26] studied the formation of parametric waves, observed only in a very dissipative medium and showing a wavelength saturation at high frequency. Melo et al [27] observed the formation of surface patterns such as stripes, squares or hexagons, due to a parametric excitation of the layer, just as in experiments with fluids [28]. The transitions between these patterns were well characterized by the relative acceleration, and were understood as a combination of period-doubling, parametric instability and subharmonic response. Recently, Metcalf et al [29] observed also a gas effect on the onset of wave formation.

At the opposite of fluidization or waves which require a strong agitation of grains, the bed can be made to compact itself when the vibration induces small fluctuations of the particles positions. Compaction of particles has been studied for its wide application, ranging from the ceramic ware [30] to the loading of packed towers [31]. One of the first complete works on this subject was published in 1930 by Westman et al [32] where mixtures of particles were studied. Idealized mixtures of spherical particles have been used by Ayer et al [33] to determine the effects on size ratio on compacity, but the difficulties encountered lead to use simply uniform spheres. In 1969, Owe Berg et al [34] found that a bed of uniform steel spheres could be compacted in a hexagonal structure provided that the vibration applied is three-dimensional. Recently Knight et al [35] were able to make some comparisons between the experimental time evolution of density and a model proposed by Barker et al [36].

2.3 Experimental Observations of Segregation in Vibrated Beds

Mixtures of particles with different properties are known to segregate when handled, particle with similar properties tending to collect together in some part of the system. The properties which can lead to such segregation include the density, size, shape and surface properties of the particles.

One of the first explanation of segregation was proposed by Weymouth [37] in 1933. Interested in the study of concrete, he varied the proportions of materials in a binary mixture of sand and pebbles and observed how the packing was affected. When the proportion of pebbles is such that the void space between two consecutive grains is smaller than the size of one grain of sand, segregation is observed simply by stirring the mixture. The cause of segregation was attributed to the large voids fraction of the packing when only small proportions of sand are mixed with pebbles. In 1939, R. L. Brown [38] also suggested that the mechanism of segregation under vibration occurs because of locally abnormal packing conditions in the neighborhood of large particles.

Between 1964 and 1965, J. L. Olsen, E. G. Rippie and M. D. Faiman published fundamental studies of segregation parameters [39-40-41]. Steel or glass spheres are vertically vibrated in a cylindrical container. Binary and ternary mixtures of various composition are prepared by changing the size, density and amount of particles. Any given mixture is observed to reach an equilibrium state whatever is its initial state. In a segregated state, the large spheres are on the top and the small at the bottom. The rate of segregation is observed to increase with the ratio of particle size in binary mixtures. Binary mixtures of particles differing only in density do not segregate. When the small spheres are denser than the large ones, segregation is much faster than when the large spheres are denser than the small ones. The segregation process is considered analogous to a reversible chemical equilibrium, with a rate constant of segregation and one of mixing. The variation of rate constants with amplitude and frequency suggest to the authors an analogy between the granular agitation and molecular temperature. The energy transfer in the granular depends on the spheres inelastic properties, and this must have an effect on segregation.

In 1963, J. C. Williams [42] performed experiments showing that the effect of size is dominant. If a large metal ball is placed at the bottom of a container filled with sand and subsequently shaken, it will be found that the ball appears on the surface of the sand, despite the fact that the density of the metal sphere is about four times that of the sand. In fact, the density of the ball has little effect on the process. A table tennis ball filled with mercury and one empty will both rise. Williams was not surprised to see rising a sphere less dense than the bed particles because he was thinking in terms of hydrostatics. However, the comparison is not straight; the ball will never move if the container is not shaken, while in a liquid, the ball moves spontaneously upward, pushed by Archimedes force, which results from the variation of hydrostatic pressure with height. In the case of a sphere more dense than the bed, he considered that the vibration creates a field of pressure increasing with the bed depth and that the weight of the large ball induces locally an additional pressure on the particles below it. Then he concludes that the mobility of the spheres below the ball is small such that a “stationary mass of particles forms” and grows each time a void allows particles to go beneath the ball.

In 1973, K. Ahmad and I. J. Smalley [43] described quantitatively some of the parameters which affect the motion of a single large particle through a dry granular bed. A wide range of frequencies 50-150 Hz and of accelerations 1-10 g was selected. The large ball was introduced at the base of a cylindrical container vibrated vertically and filled with a known height of sand. It was found that at a constant frequency of vibration, the rise velocity increased with increase in acceleration; however, at a constant acceleration, rise velocity was decreased with increase in frequency. It was also shortly concluded that the rise time increases with increase in bed depth, particle density and size, and depends on the particle shape.

In 1993, J. B. Knight [15] proposed that the vibration-induced rise of the large sphere arises from convective processes. A cylinder was filled with glass beads and one larger glass sphere. A tracer technique was used to visualize the flow. It was observed that an inner core of beads together with the sphere travels to the bed surface. After reaching the top, the small background beads move towards the outer walls and begin to move along the walls towards the bottom of the cylinder. Because the width of the downward

flow is small, a sphere too large will be trapped on the surface, resulting in size segregation. The convective flow pattern exists if there are frictional contacts between the beads and the walls, and the flow direction can be reversed if the walls slant outwards from the base. Additional results show that the rise velocity increases when the beads get closer to the surface. A much more detailed study of the convective flow has been carried by the same authors recently [16].

The influence of size ratio (intruder diameter relative to the diameter of a bed particle) has been observed in a two-dimensional bed by Duran et al [44]. They used a container made of two rectangular glass plates separated by rectangular plastic wedges. The oxidized aluminum balls used in this experiment have a high solid friction coefficient at the lateral walls and high momentum loss on collision. The pile is prepared to match as closely as possible a compact triangular lattice, except around the intruder that induces local perturbations in the array. Convection rolls associated with heaping show up when the cell is shaken with relative accelerations between 1 and 2. At $\Gamma = 2$, the intruder is carried by a convection flow of the small balls. But at $\Gamma = 1.25$, the rise velocity is dependent on the intruder diameter. Typically, the rise velocity increases linearly with the intruder diameter. For small diameters, an intermittent rise is observed, i.e. the trajectory of the intruder shows period of time with rise and period of time with rest. The authors also observed density microfluctuations inside the bulk, occurring during the free flight of the bed. These fluctuations take the form of cracks, i.e. a rupture along an irregular path between two dense phase. It was hypothesized that cracks could be a leading mechanism for the motion of the intruder. The same authors introduced an arching effect model [45], which describes the existence of a critical size ratio separating a regime where the rise is intermittent from a regime where the rise is continuous. First, they show the existence of arches or vaults which sustain the intruder from the sides while the balls laying beneath the intruder are not in contact with itself. When the intruder is lifted up, the bed geometry changes and the intruder find a stable position whenever vault clamping occurs. The distribution of stable positions along height is shown to depend on the size ratio. There is a critical size ratio separating a discrete and a continuous distribution of vaults, which is thought to be the same than the one separating intermittent and continuous rise.

The influence of size ratio has also been observed by Cooke et al. [46] with an experimental set-up mainly identical to the one used by Duran et al. However, Cooke et al. came up with a different interpretation of the ball rise. When a crack occurs, a global upwards shift of the surrounding balls pushes from below the intruder. From this fact, the conclusion is that the rise mechanism is convective since the intruder rises at the same speed than the particles around it. Nonetheless, Cooke et al observed also a size dependent rise velocity, a priori in contradiction with the features of a convective flow. The difficulty is avoided by considering that the frequency of the density fluctuations (which create the cracks) depends on the size of the intruder, such that the larger is the intruder, the more perturbed is the regular lattice of background particles, the more often cracks occur and the faster is the rise. Eventually, the frequency spectrum of the intermittent and continuous rise regimes are very similar, which suggests to the authors that there is no fundamental difference between the two regimes.

Note that all the experimental works described here make few connections between all the possible behaviors presented in 1.2.2 and the rising phenomenon.

2.4 The Contribution of Computer Simulations

With the extraordinary development of workstation ten years ago, simulations became a way for scientists to study granular properties that are usually very difficult to observe experimentally. Of course, simulations do not replace experiments, but are a good tool to test our understanding of phenomena by finding the minimum necessary ingredients to describe them. The following review of simulations focuses on the rise of a large sphere.

In 1986, P. K. Haff et al [47] performed molecular-dynamics simulations and identified a segregation mechanism associated with shear motion in a two-dimensional bed of inelastic frictional disks. Simulation results show that it is difficult to make a large disk rise in a box with vertical walls, vibrated both vertically and horizontally. If the horizontal vibration is chosen properly or if inclined walls are used, the segregation strength is significantly increased. The large disk is observed to roll up over adjacent smaller particles. In this process, the friction between the large disk and the bed particles must be large enough.

Almost at the same time, A. Rosato et al [48-49] conducted simulations based on an adaptation of the Monte-Carlo method. In a two-dimensional system, shaking is modeled as a process in which all the particles are first lifted and then dropped to the bottom of the container. The effect of interparticle collisions, collisions with the walls, and the slight horizontal jostlings of the container are modeled as random movements of the particles with respect to one another. The segregation mechanism is described as follow :

- (1) as the particles fall during a shake, small particles easily move in beneath a large particle whenever gaps open up;
- (2) a large particle may move back down if many small particles simultaneously move from beneath it;
- (3) this is an unlikely event, and therefore large particles move up relative to small particles.

Thus, segregation is the consequence of a geometrical effect. Other results show that the rise of the large disk is approximately linear and that the rise velocity increases with the size of the large disk as well as with the shaking amplitude. Also, anticipating the results of future experimental works, it is observed that at small shaking amplitudes (smaller than about one quarter the small particle size) the disk motion occurs in a step-like-jumps, with the step approximately equal to the height of one row of small particles.

R. Jullien et al [50] presented three-dimensional simulations where a deposition algorithm leads to size segregation. Particles are dropped, one at a time, via randomly located vertical trajectories onto a horizontal substrate where they form a deposit. After they contact the deposit, they follow the path of steepest descent until either they reach a local minimum on the surface of the deposit or they contact the substrate. At this stage, particles are incorporated irreversibly in the growing deposit. Initially used to model segregation when pouring a heap [51], this algorithm can be used to simulate the rise of a large sphere. During the deposition process, a hole forms below the large particle. At the next deposition cycle (or shake), some small spheres fall in the hole and the large sphere is consequently raised. The mechanism described is similar to the one proposed by Rosato et al. Then, it is not very surprising that the rise trajectory is linear. In addition, there is a critical size ratio Φ_c below which the large ball will stop its rise at an height of a few small particle diameters. It is shown that Φ_c depends on the angle of repose of the granular, which has an effect on the shape of the hole [52].

S. Dippel et al [53] used a modified version of the algorithm introduced by Rosato et al [45-46] to compare with segregation experiments at low vibration amplitude. The simulations show avalanches of small particles falling in a very stable triangular hole below the large particle. The averaged rise speed is observed to vary with Φ irregularly and not linearly like in experiments [41].

G. C. Barker et al [54] criticized the relevance of the critical size ratio Φ_c found by R. Jullien et al [47], as a result of sequential and deterministic simulations of segregation. Collective behavior of particles, such as the formation of arches or bridges, and non-deterministic effects due to the complex coupling with the vibration can be reproduced in simulations involving a combination of Monte Carlo dynamics and non-sequential random close packing [55-56]. In such simulations, no critical size ratio is observed [57].

T. Ohtsuki et al [58] performed molecular dynamics simulations of inelastic hard disks to study the influence of particle size and density. In all cases, the large particle reaches an asymptotic height independent of initial positions. When the size ratio is smaller than one, no rise is observed. When the size ratio is bigger than one, the ball rises if the density is small enough; if the density is about five times the density of the bed particles, the ball does not rise.

Y. Taguchi [59] and J. A. C. Gallas et al [60] were able to obtain simulations of granular convection. Afterwards, T. Pöschel et al [61] studied the effect of convection on the rise of a large sphere by molecular-dynamics simulations of a two-dimensional bed. The particles have a radii uniformly distributed between $\pm 15\%$ of the average radius and the large sphere is four times larger than the average radius. There is a characteristic frequency above which convection starts and below which only fluctuations are observed. This characteristic frequency depends on the initial depth of the large particle. Whenever segregation is observed, it is associated with convection. At the convective transition, the presence of the large particle increases the strength of convection comparatively to the case without the large particle. This effect is thought to be related to the fact that “in the region around the large particle, the accelerations are higher because the momentum is transferred with less dissipative loss through the larger particle than through a corresponding pile of smaller particles with the same volume”. When the size ratio is

decreased, the large particle goes up and down in a “whale effect”, apparently following the convection rolls. An extension of this work has been done by J. A. C. Gallas et al [62] in a three-dimensional system. The “whale effect” is again observed and presented as a consequence of an increase in convection strength coupled with a decrease in bed compacity. Also, changes in dynamic behavior are observed when the energy dissipation is modified.

Y. Lan et al [63] used the discrete element method to simulate convection and observed the effects on a large sphere. A thin cell with periodic boundaries represents the container. Surprisingly, the ascent speed increased when the coefficient of restitution was decreased. A small sphere just below the large sphere and the large sphere itself are observed to have almost the same history of displacements and velocities, indicating the convective nature of the rise. The “whale effect” is observed only when the width of the cell is large enough.

2.5 Motivation

Many questions concerning the mechanism of segregation are still open. Most of the experiments show that convection is the driving force [15-41-43], but Duran et al were able to observe a non-convective rise [41]. Simulations described either a convective rise or the geometrical mechanisms involved in a non-convective rise, but never both. The role played by the size ratio Φ is particularly unclear. The “whale effect” has never been described experimentally. A major problem is that the basic behavior of a vibrated bed of uniform particles is already very rich (as described in 1.2.2) and that this complex phenomenology has never been related to the ubiquitous segregation effect. As pointed out by G. C. Barker et al [64], “the competing domains of amplitude and frequency need to be investigated experimentally in order to find better control parameters”. The aim of this thesis is precisely to explore the vibration domain as fully as possible hoping that it will give a better understanding of the segregation process.

CHAPTER 3

EXPERIMENTAL PROCEDURES

3.1 Objective of the Experiment

The experiment is designed for the observation of a large ball rising in a vibrated granular medium. Two different approaches are adopted. In the first one, the trajectory of the ball in the medium is recorded by using a tracking system, which allows the determination of the position and the rotation of the ball. This approach could be called Lagrangian since it consists in following the motion of a given particle in the granular material. In the second approach, the observation is restricted to the location on the surface where the ball finally emerges. This emergence is characterized by the time it takes for the ball to go there from an initial position. The second approach is Eulerian since we always look at the same spatial location of the granular material. In all the performed experiments, the ball is placed at the center of the bottom plate. Other initial positions are not considered in order to focus on an elementary understanding of the rise time dependence on the vibration parameters. The influence of the initial height or radial position is beyond the scope of this thesis. Results concerning the effect of initial position are described in recent publication [46].

In addition to the analysis of the sphere's rise, an observation of the global bed response to the input vibration is carried. When a wide range of excitation parameters is involved, it is possible to observe most of the common features displayed by a vibrated granular bed, such as heaping, subharmonic instabilities such as arching, surface waves, convection, fluidization or compaction. The apparent bed behavior is observed visually, sometimes with the help of a stroboscope and sometimes by following the motion of tracers. The synthesis of the complementary observations of the ball motion and the bed behavior will be presented in Chapter 6.

An important goal of the investigation is to find the relevant vibration parameters able to properly describe the segregation process. The obvious parameters are the amplitude and the frequency, but the vibration velocity or the relative acceleration are two other parameters which may be meaningful. Consequently, series of measurements have

been made by fixing either the amplitude, the frequency, the velocity or the relative acceleration and varying the three remaining parameters. Hence, there are twelve possible combinations of fixed and variable parameters. It appeared that the most interesting cases are the variation of rise time with frequency and amplitude at fixed relative acceleration, and the variation of rise time with relative acceleration at fixed amplitude or fixed frequency.

3.2 Description of the Experimental Setup

The granular bed is made with monodisperse acrylic spheres. The spheres fill a cylindrical container whose walls are made of plexiglass and whose floor is a piston. The piston is mounted on a vibration exciter which is a combination of a B&K[†] general purpose head type 4812 and a B&K exciter body type 4801. The vibration exciter is driven by a B&K power amplifier type 2707. An accelerometer B&K is fixed on the piston base and is connected to a B&K vibration exciter control type 1050. The vibration exciter control is a device containing a digitally controlled generator which provides an input signal to the power amplifier, a vibration meter enabling accurate measurement and control of any vibration parameter, and a compressor for regulation of the vibration exciter excitation. During an experiment, the vibration exciter control permits an easy variation of the vibration frequency at fixed amplitude, velocity or acceleration.

A granular bed is a complex material. Its properties are very dependent on the environment and are not easily predictable. The temperature and the humidity level in the room have significant effects on the bed response. It is important to be able to control these parameters. A fan is used to reduce the temperature increase caused by heating of the vibration exciter while an air conditioner helps to reduce the humidity level in the room. A digital meter gives measurements of the temperature and humidity. In Chapter 4, the effects of temperature on the measurements will be discussed. Another undesirable event is the formation of static electricity on the particles' surface created by the numerous collisions during shaking. When the particles are charged, they repel each other and usually stick on the container walls whose charge is opposite. Then, the particle-particle and wall-

[†] Bruel & Kjaer

particle interactions are not simply frictional or collisional interactions, but also include long distance electrostatic interactions, which are too difficult to master and can lead to the disparition of previously observed behaviors. To avoid the build-up of static electricity, the particles are treated with an anti-static sheet, used usually to prevent the formation of static cling on clothes. After several months, this treatment is still effective.

For most of the experiments, the large ball used is the one specially designed for the tracking system as detailed in section 3.4. In some cases, to study the dependence on the large ball size, other spheres of the same material as the bed particles are used.

3.3 Experimental Parameters

The cylinder has a diameter D_{cyl} of 4.5 ". The diameter of the piston is slightly smaller so that it can move without rubbing on the cylinder's walls. The bed particles have a diameter $d = 1/8$ ". The initial bed depth H is smaller than D_{cyl} , so that the bed aspect ratio H/D_{cyl} is smaller than unity. The results are obtained for $H/D_{\text{cyl}} = 0.44$. The bed is rather shallow so that bulk and surface phenomena are likely to interact strongly. The bed particles have a low coefficient of friction, estimated at about 0.2, and a high coefficient of resitution, greater than 0.9. To measure the coefficient of friction, three balls are stuck together, deposited on a plexiglass surface which is raised to determine the angle of static friction. The large ball to bed particles size ratio is defined as $\Phi = D/d$, where D is the large ball diameter, and varies from 1 to 12. The large ball is placed initially at the center of the piston surface and is usually seen to remain centered during its rise. The temperature and humidity of the room are noted before starting to shake the piston. A sinusoidal vibration $a \sin(\omega t)$ is applied to the piston, where $\omega = 2\pi f$. The frequency f has been varied between 5 and 75 Hz. The highest amplitude the vibration exciter can provide is $a = 0.25$ ", or equivalently $a = 2d$. Commonly used as a control parameter in vibrated granular experiments, the relative acceleration Γ is defined as the ratio of the maximum vibration acceleration to gravity, i.e. $\Gamma = a\omega^2 / g$. With the amplitudes and frequencies used, values of Γ ranged between 0 and 13.

3.4 Measurement Techniques

3.4.1 Tracking system

A non-intrusive tracking system developed at the Particle Technology Center [65-66-67-68] can be used to find the three-dimensional position and rotation of the large ball during its rise in a nontransparent bed. The technique is based on the principle of magnetic induction coupling. The particle being tracked contains three small perpendicular transmitters, associated electronics and a battery. The experimental space is surrounded by receiving loop antennae, in each of which voltages are induced due to the coupling between the transmitters and the antennae. From these voltage readings, the three dimensional position and orientation of the tracked particle is determined. A picture of the antennae surrounding the experimental system is shown in Fig. 3.1.

Before running an experiment, the ball to be tracked must go through calibration procedures. The ball is placed in the middle of the antennae cage, is oriented such that each transmitter is successively perpendicular to each antennae, and the corresponding voltages are measured. Because the transmitters are perpendicular to each other, only four positions of the ball, also called correlation points, need to be recorded. When this has been completed, the bed is vibrated and the acquisition of the induced voltages is started. Due to the limited lifetime of the battery, experiments longer than 20 minutes are not possible without uncontrollable loss of accuracy. Once the acquisition is stopped, the data is processed using a software designed to compute the coordinates of the ball. The correlation points are used as a reference for the calculation, and the user can modify the coordinates system through the definition the antennae' position. Eventually, the three-dimensional trajectory of the ball can be plotted as a function of time.

The computation time required for processing is long. In average, it was possible to obtain one complete position per second. Furthermore, the acquisition rate is of about 900 Hz, which means that one second of experiment will be processed in about 15 mn. When the observed phenomenon last for several minutes or even hours, it becomes impracticable to use the tracking system. At the writing of this thesis, improvements designed to reduce the acquisition rate are under construction.

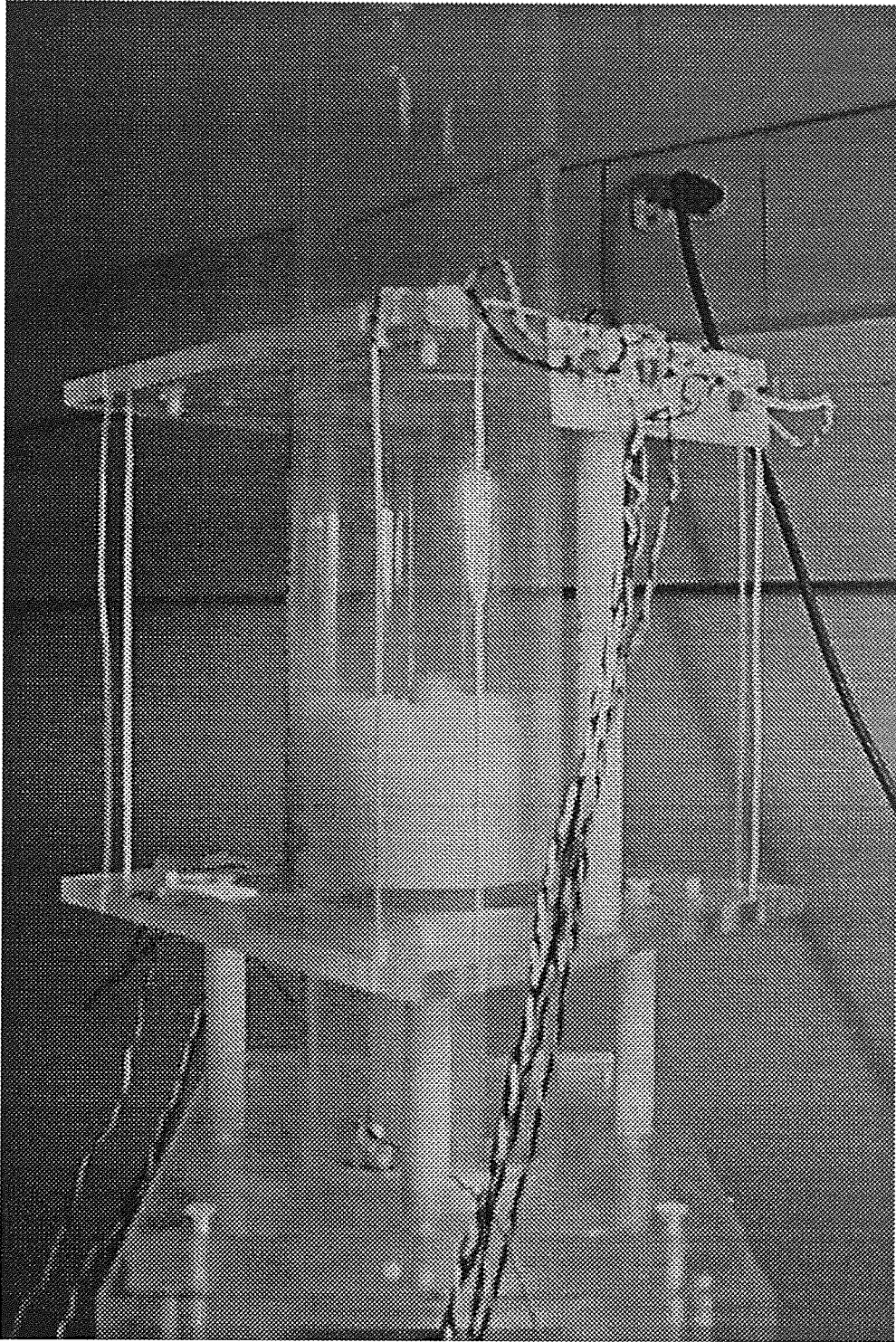


Figure 3.1. Granular bed surrounded by an antennae cage.

The shell constituting the external part of the ball is made of polyethylene. Although this material is not the same as the bed particles', only small deviations in the results have been observed when comparing with an acrylic ball of the same size. Besides the surface properties, the density of the ball can change the results. Due to the structure of the tracking ball, its density is inhomogeneous and larger than the density of the bed particles. The inhomogeneity of the ball density makes it difficult to interpret the rotations observed, which could be attributed either to an effect of the ball unbalance or to the physical mechanism causing the ball to rise.

3.4.2 Use of a Simple Device: The Stopwatch

When our knowledge of things is inadequate, it is often productive to simplify the problem. Instead of looking for a complete description of the ball motion at given vibration parameters, we can study the variation with the vibration parameters of a single variable, the rise time, characteristic of the average ball motion. The rise time is a measure of the time the large ball will need to go from its initial position to the bed surface after the vibration starts. A simple tool to measure the rise time is the stopwatch. When the vibration starts, we start the stopwatch, and when the ball reaches the surface, we stop the stopwatch. The time when the vibration starts is well defined, but the time when the ball reaches the surface depends on the criterion used. Three different times has been considered. There is a time when the top of the ball just reaches the level of the bed surface. There is a time when the ball is half in the bed, half outside. There is also a time when the ball reaches its highest altitude above the piston floor. In general, the last criterion is used to determine the rise time. When more appropriate, the first or second criterion is employed, and this will be explicitly mentioned in the text.

CHAPTER 4

RESULTS: STUDY OF THE RISE TIME

This chapter begins with a discussion on the problems encountered to obtain repeatable results. The main part of the results is the identification of several rise regimes. One of the regimes can be described using a new non-dimensional parameter, which appears as a necessary scaling parameter to connect with the results of Ahmad et al [43]. The role of the usual non-dimensional acceleration or relative acceleration is also addressed.

4.1 Limitations

The results presented in this chapter are limited by the fact that measurements are very sensitive to the experimental conditions. Structural disorder, external parameters such as temperature or humidity, internal parameters such as bead-bead or bead-wall friction have all a contribution very ill-defined and often fluctuating with time.

Interparticle contacts are known to create a disordered network. This effect is attributed mainly to inhomogeneity in size or shape between particles, as small as these inhomogeneities might be. The straightforward consequence of this disorder is the remarkable difficulty to understand the equilibrium of a simple sandpile. In a dynamical situation, how much can contacts disorder affect the behavior of the granular ? This question has to our knowledge no answers. When submitted to a strong forcing, a granular loses quickly the memory of its earlier configurations. Then, the common hope is that the macroscopic behavior depends only on an average of local properties. In this case, the initial configuration of the bed structure should have little effect on the outcome of the vibration process. In fact, it is very often the case in systems with large degrees of freedom as pointed out by Cross et al [69]. However, it has been judged important to prepare the bed the same way for all experiments. The bed was obtained by pouring gently the spheres on the surface of the piston so that the resulting packing is loose.

During the early steps of the investigation, it appeared that it was difficult to obtain repeatable results, from one day to the other. A more attentive observation finally lead to the conclusion that temperature fluctuations and humidity can have a strong effect on the

bed response to vibration. For example, it was striking that at the end of a day the convection strength was much lower than in the morning for the same experiment, and that at the beginning of the following day, convection was recovering its original strength. In fact, after a long time, the heat released by the vibration system may increase the room temperature of about 5°C while over night, the vibration system cools down. Fig. 4.1 shows the rise time measured when $f = 20$ Hz and $\Gamma = 4$ for 56 runs:

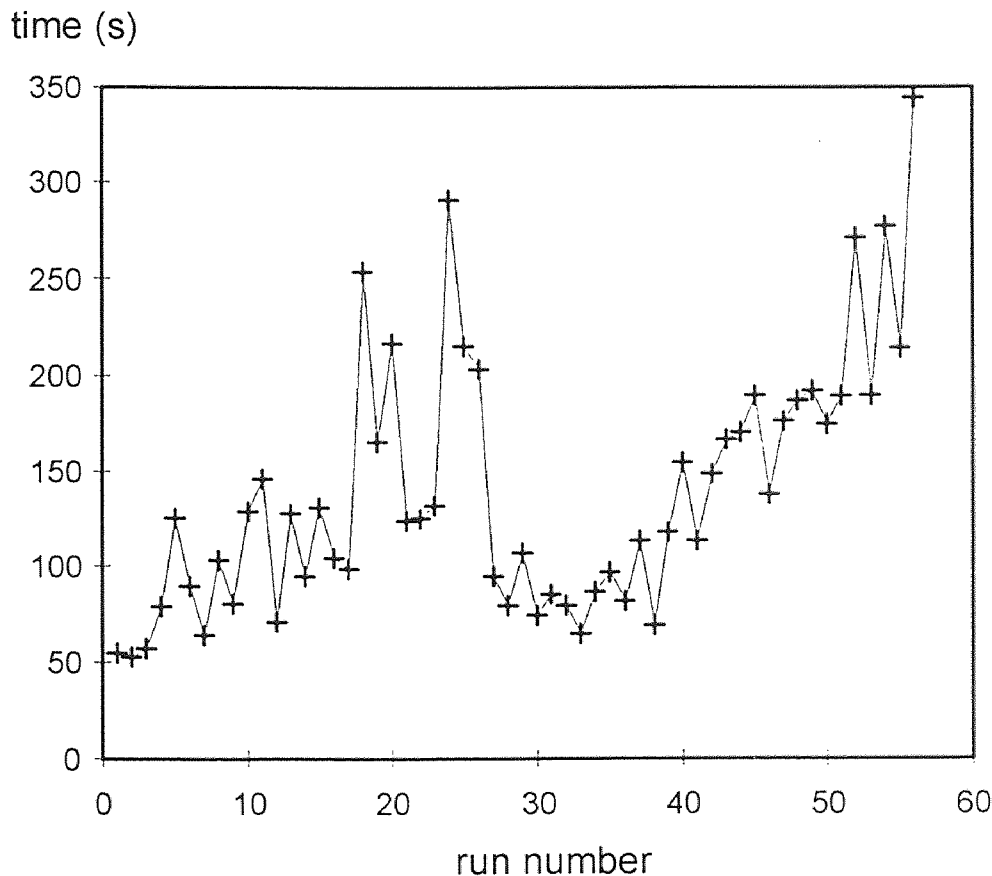


Figure 4.1. Successive measurements of rise time for fixed vibration conditions.

After the first consecutive 27 runs, the vibration system is allowed to cool down during 2 hours, and then 29 other consecutive runs are performed. Despite the large fluctuations observed, there is a clear tendency of the rise time to increase with the number of runs performed. After the system cools down, the values of rise time are much lower than

before but again, there is an increase with the experiment number. Some repeated measurements of rise time and the corresponding room temperature have been made in order to clarify the role of temperature on the rise time. The bed is now vibrated at $f = 12$ Hz and $\Gamma = 4$. In Fig. 4.2, room temperature and rise time are plotted on the same graph as a function of the experiment number:

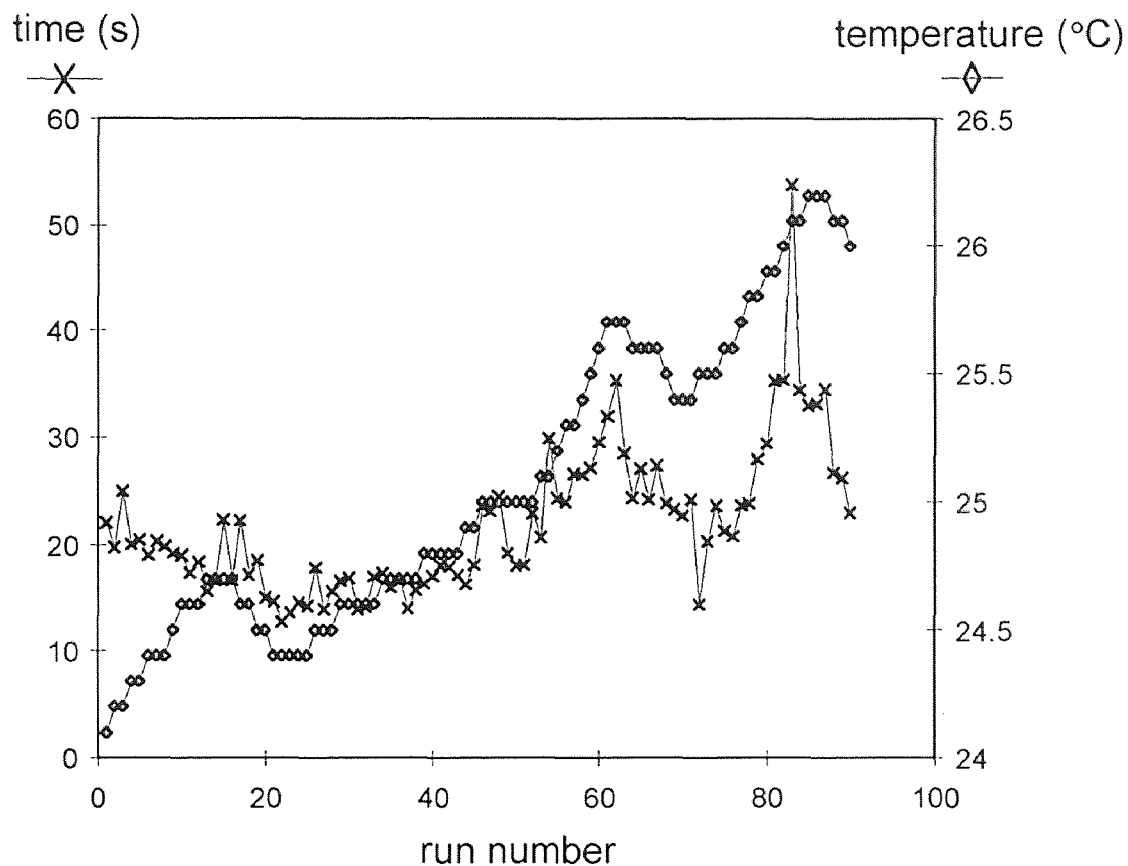


Figure 4.2. Correlations between temperature and rise time fluctuations.

While the variation in temperature is only of about 2°C , the rise time varies between about 10s and 50s. Moreover, the fluctuations of rise time follow approximately the fluctuations of temperature, except during the first 10 runs. Thus, we conclude with some confidence that temperature has a very significant effect on our results. Consequently, as already mentioned in chapter 2, a fan has been used to reduce the effect of temperature

fluctuations on the experiment. The reason why temperature is so important is not clear. For example, a change in temperature may affect the contact properties or the size of grains due to dilatation. The effect of humidity has also been observed. An increase in humidity leads to a longer rise time. When humidity is high, the water adsorbed on the particles' surface change the contact properties, and the granular cannot be considered as dry anymore. The control of temperature as well as humidity is a crucial issue that we were able to address only partially by approximate methods. It deserves certainly a better attention.

Convection in a granular bed composed of sufficiently large particles is strongly dependent on the amount of friction at the walls, as many authors already mentioned [16,18]. One problem is that the surface of the wall can easily be damaged by the rubbing of bed particles and its frictional properties will be altered. One solution is to cover the wall with particles stuck on its surface so that the rugosity will remain high and hopefully stable for a long period of time. This technique has also the advantage to enhance the frictional mechanism of convection. Unfortunately, it was not possible to apply easily this technique to our experiment since the piston need to slide along the wall, close enough to prevent particles from falling but without hitting the wall coating. The control of wall friction is consequently very poor.

4.2 Rise Regimes

If the rise time T is plotted as a function of frequency for several values of fixed relative acceleration, it is possible to distinguish three main domains, where the rise time variation is different. In fact, it was chosen to plot Tf , i.e., the rise time dimensioned by the frequency, which physically measures the number of vibration cycle applied. We stress out that this choice does not change the qualitative features observed. Each variation domain corresponds to a different macroscopic behavior of the bed. The regimes have been classified according to the observed behaviors: heaping and convection, convection in the absence of heaping, and crystallization.

4.2.1 First Regime: Heaping and Convection

Heaping has been observed only for low frequencies when $f < 15 \pm 1$ Hz. In Fig. 4.3, Tf is plotted on a logarithmic scale as a function of frequency and the curves correspond to a fixed relative acceleration.

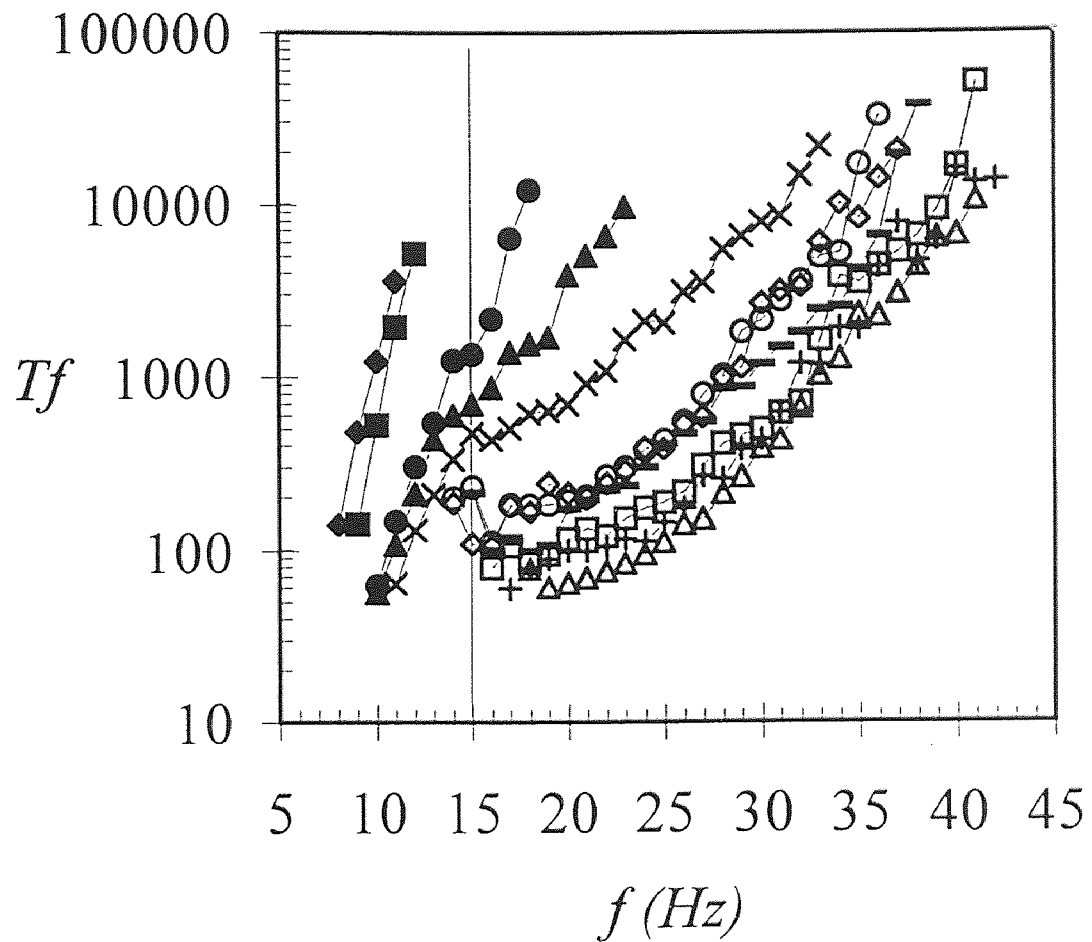


Figure 4.3. Dimensionless rise time Tf as a function of frequency f , for a range of relative acceleration Γ : (\blacklozenge) = 1.5, (\blacksquare) = 2, (\bullet) = 2.5, (\blacktriangle) = 3, (\times) = 3.5, (\circ) = 4.5, (\diamond) = 5, (\blacksquare) = 6, (\square) = 7, ($+$) = 8, (\triangle) = 9. The vertical line delimits the first and second regime. Each curve connects data of same Γ .

When $f < 15 \pm 1$ Hz and at fixed acceleration, the logarithm of Tf increases linearly with f . The curves obtained when the acceleration is varied, stay mainly parallel to each other. The data can be fitted with a linear law as:

$$\ln(Tf) = \alpha(\Gamma)f + \beta(\Gamma)$$

The coefficient $\alpha(\Gamma)$ is a constant almost equal to unity for $1.5 < \Gamma < 3.5$. The coefficient $\beta(\Gamma)$ is very small, but its value describes the variation of Tf with Γ . When f is fixed, Tf decreases with Γ , as well as $\beta(\Gamma)$.

In this first regime, a strong internal convective flow, coupled with surface avalanches, carries the intruder upwards. The increase of rise time is associated with a decrease in the convective speed. When the frequency is close to 15 Hz, the flow is very slow. Then, the heap is seen to start near the walls and to expand towards the middle of the cylinder in a similar way than the two-dimensional observations of Clement et al. [16]. Heaping has also been observed when $\Gamma < 1$, which is rather unusual. Indeed, the heaping threshold most commonly reported in the literature is $\Gamma \cong 1.2$. The reason why heaping has been observed below this value is quite simple. If a piston continuously pushes upward a granular bed and if there is enough friction on the side walls, then heaping associated with convective rolls is forming (private communication). The imposed relative motion between the bed and the fixed walls creates a shearing force responsible for that. When a vibration is applied, heaping will be seen as soon as a relative motion between the bed and the walls occurs. If the walls are fixed, there will always be relative motion, while if the whole container moves, relative motion occurs when the bed starts to fly, which is possible only if $\Gamma > 1$.

4.2.2 Second Regime: Convection in the Absence of Heaping

The second regime is observed for $f > 15$ Hz, where there is no more heaping. The top surface is flat but observations of the bulk motion show that convection still exists. A black tracer, introduced in the bed and placed at the center of the container, will rise and move towards the wall; then it will go down along the wall, move away from the wall at an undetermined depth and some time later will appear again on the top surface. The

width of the downward flow is of 2 to 3 bed particles' diameter. The large sphere is carried towards the walls by the flow but stay on the bed surface, obviously because the width of the downward flow is too small.

The rise time variation is now different from what was observed in the first regime. Fig. 4.3 shows that the rise time on curves of fixed relative acceleration, varies slowly close to $f = 15$ Hz, but increases faster and faster as frequency is increased. For $\Gamma = 2.5, 3$ and 3.5 , the rupture between the first and second regime is clearly pictured by the change in shape of the rise time curves before and after the transition. Like in the first regime, at fixed frequency, there is a general decrease of Tf when Γ is decreased.

For $\Gamma \geq 3.5$, the curves have all essentially the same shape. The following equations have been used to fit the curves:

$$Tf = \frac{\alpha}{[\Gamma - \Gamma_c]^\beta} \left[\exp\left(\frac{f}{f_c}\right)^2 - 1 \right] \quad (1)$$

and

$$Tf = \frac{\alpha}{[\Gamma - \Gamma_c]^\beta} \exp\left(\frac{f}{f_c} - 1\right)^2 \quad (2)$$

The form of equation (1) is a simplified version of Knight et al. phenomenological law [19]. Equation (2) has been introduced to account for the fact that, close to the transition, the rise time varies slowly. Indeed, equation (2) expresses clearly the additional condition that $d(Tf)/dt = 0$ for $f = f_c$, where f_c is expected to be close to 15 Hz. Both equations agree with the fact that the shape of the curves is independent of Γ , i.e. f_c is a constant, and the fact that at fixed frequency, Tf decreases with Γ , whose variation is given by the term $[\Gamma - \Gamma_c]^{-\beta}$. Equation (1) is well fitted when $\Gamma_c \cong 1$, $f_c \cong 15.7$ Hz, $\beta \cong 1.39$ and $\alpha \cong 300$. It is very interesting to note that the value of f_c corresponds quite well to the demarcation between the regimes with and without surface heaping. Equation (2) is well fitted when $\Gamma_c \cong 1$, $f_c \cong 11.7$ Hz, $\beta \cong 1.21$ and $\alpha \cong 570$. In this case, the value of f_c underestimates the frequency of transition. The exponent β describing the decreasing behavior is similar in both fits.

The original phenomenological law proposed by Knight et al. [19] is:

$$Tf = \tau \left[\exp\left(\frac{H}{\xi}\right) - 1 \right] \quad (3)$$

where it was found that:

$$\tau = \frac{\alpha}{[\Gamma - \Gamma_c]^\beta} \exp(\gamma f + \delta) \text{ and } \xi = \frac{1}{\varepsilon f^2 + \lambda}.$$

Equation (3) has initially been used to fit the data of Fig. 4.3. However, it appeared that many of the parameters (γ , δ , λ) were negligible and that ε was independent of Γ , in contrast with Ref. [19]. This is the reason why equation (1) has been used instead of equation (3). Several characteristics of the experimental procedure we used may be at the origin of the different scaling:

1. The walls are fixed, while in Ref. [19] the walls move with container.
2. The vibration is continuous, while in Ref. [19] taps followed by rest time were applied.
3. The bed aspect ratio is smaller than unity ($H/D_{cyl} = 0.44$), while in Ref. [19] it is bigger than unity ($H/D_{cyl} = 1, 2, \text{ and } 3$).
4. The bed depth is $H/d = 12$, and MRI experiments in Ref. [19] show that the top 10 to 15 layers do not follow well equation (3).

However, despite the differences between the two experiments, both scalings obtained with equation (1) and (3), contain a contribution growing like $\exp(f^2)$, which is the essential term describing the quadratic shape of the curves appearing in Fig. for $f > 15$ Hz.

4.2.3 Third Regime: Crystallization

The third regime is observed at small vibration amplitude, where there is no more convection. The first effect of the small amplitude shaking is to compact the bed. Because the bed is composed of monodisperse spheres, the initial random and loose packing reaches a very ordered state, where the structure is mainly hexagonal compact: this phenomenon will be called crystallization. Fig. 4.4 shows a view from the top of the bed where the “crystal” structure is clearly seen. Most of the particles are frozen in position by the structure, but still have a significant rotational motion. There are still very small

convection rolls at the walls, where particles are either absorbed or ejected. Sometimes, absorbed particles are seen to follow a convection roll about $3d$ wide and $3d$ deep. Some “free” particles move randomly on the crystallized surface looking for a potential well, for example a hole in the structure or a place very close to the walls where the rolls prevent the formation of a crystal.

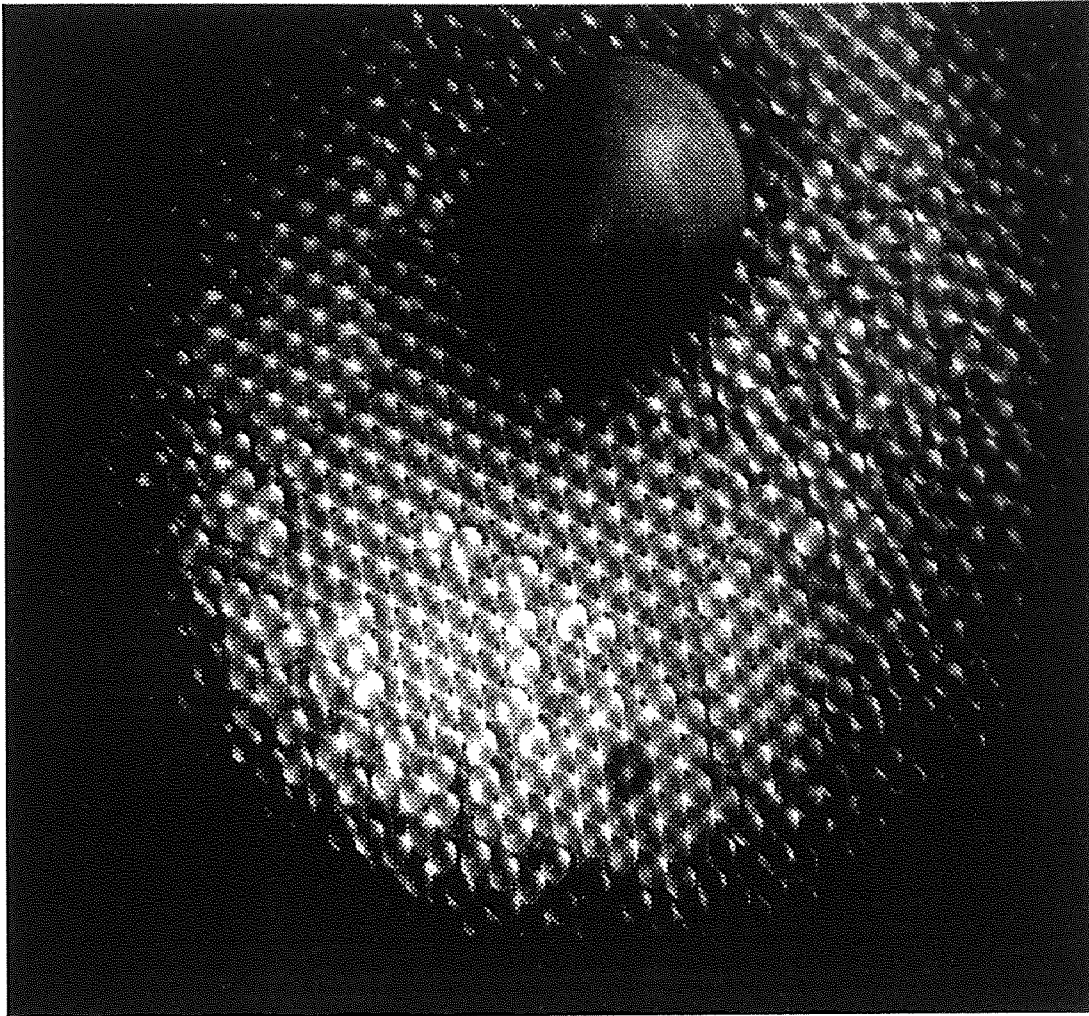


Figure 4.4. View of the top surface when the bed crystallizes. Note the regular packing typical of a hexagonal structure.

Crystallization is clearly observed when $a/d < 0.25$, that is when the amplitude is much smaller than the diameter of the bed particles. The rise time corresponding to the crystallized regime appears in the high frequency domain of Fig. 4.5, which also shows roughly the first and second regimes. For $\Gamma > 4$ and $f > 40$ Hz, the spread with Γ is minimal and the points almost lie on a straight line. Thus, like in the first regime, the rise time variation with frequency is exponential. The data can be fitted with a simple linear equation:

$$\ln(Tf) = \alpha f + \beta,$$

where α and β are independent of Γ . It was found that $\alpha = 0.107$ and $\beta = 4.02$.

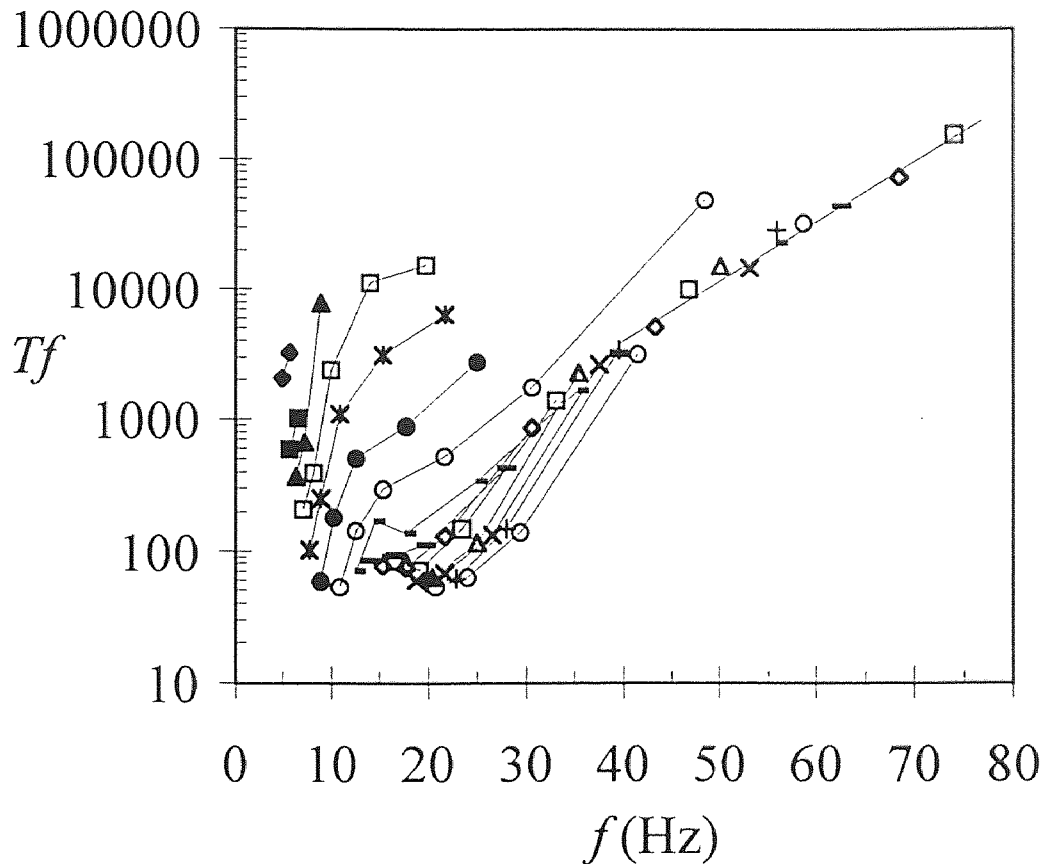


Figure 4.5. Dimensionless rise time Tf as a function of frequency f , for a range of relative acceleration Γ : (\diamond) = 0.6, (\blacksquare) = 0.8, (\blacktriangle) = 1, (\boxtimes) = 1.25, ($*$) = 1.5, (\bullet) = 2, (\otimes) = 3, (\blacksquare) = 4, (\blacksquare) = 5, (\diamond) = 6, (\square) = 7, (\triangle) = 8, (\times) = 9, ($+$) = 10, (\circ) = 11. For clarity, symbols are not connected in the third regime; only a single line shows the linear trend.

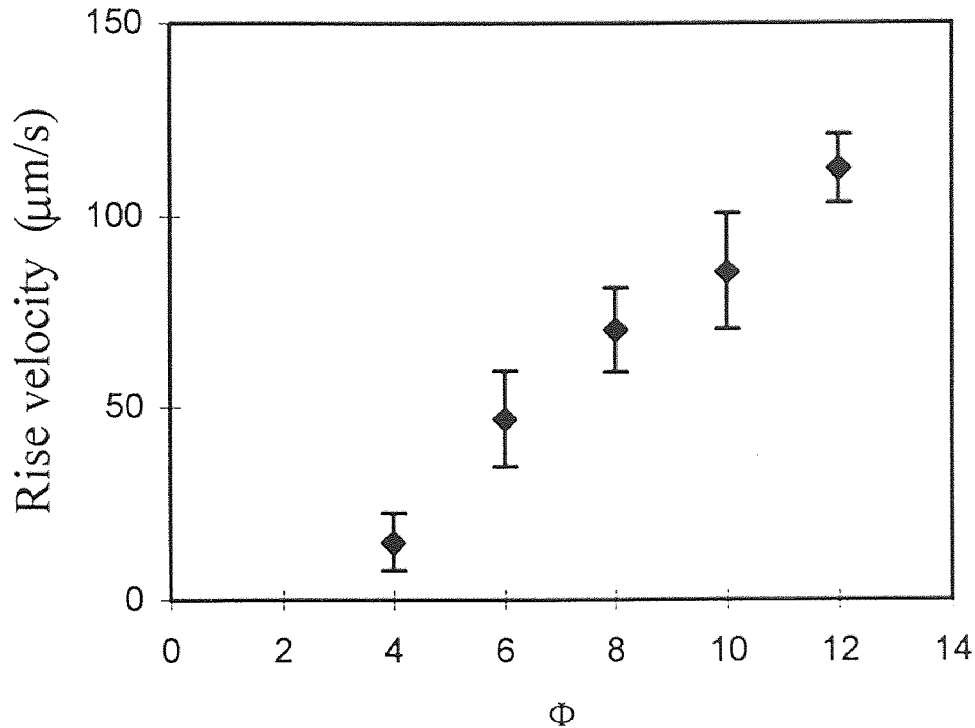


Figure 4.6. Average rise velocity ($\mu\text{m/s}$) as a function of size ratio Φ , when $f = 50$ Hz and $a/d = 0.1$.

Despite the existence of very small convection rolls, the rise mechanism is believed to be “non-convective”. A clear distinction from the convective regimes appears when one look at the motions of the particles around the intruder. Indeed, the particles are falling in the voids created below the intruder showing up on the surface, while they would rise together with the intruder in the case of a convective flow. In addition, the mean velocity of the large ball depends on the size ratio $\Phi = D/d$, as shown in Fig. 4.6, for $f = 50$ Hz and $a/d = 0.1$. The larger the ball, the faster it rises to the surface. A priori, this result is in contradiction with the occurrence of a convective flow which drags all the particles at nearly the same velocity, whatever their size, density or shape is. Previously, effects of size ratio had been seen in a two-dimensional bed [19,20], but the extension of this result to three dimensions was until now not straightforward. In a two-dimensional (2D) system,

the spheres tend naturally to pack in a triangular mesh which is not the case for a three-dimensional (3D) system. As a result, in 2D, two rising behaviors have been observed, one purely convective and the other dependent on the size ratio [19-20], while in 3D only convection has been described as the mechanism causing a large sphere to rise [8-9]. However, since it is possible to obtain a strongly ordered structure by shaking at very small amplitude in a 3D system, it is possible to observe a size ratio dependent and apparently “non-convective” regime. In 2D, this behavior is observed when an initially regular packing is sustained by using low accelerations [19]; in contrast, in 3D, the regular packing is created by the vibration itself, at low amplitude and high accelerations. Far from being in a quasistatic state, the particles fixed in position by the “crystal”, still have a significant rotational motion. Thus, they can feel the repeated action of their neighbors and may eventually feel the presence of the intruder.

4.3 Scaling Properties of the Vibration Amplitude

In order to examine the effect of vibration amplitude, the same data as in Fig. 4.3 is shown in Fig. 4.7 replotted against normalized amplitude a/d for fixed values of Γ . There is a general decay of Tf with a/d , and for Γ greater than approximately 4, the data tends to collapse on a single curve, while for $\Gamma < 4$, there is more scatter. The curve exhibits the important feature that Tf increases quickly as a/d is reduced. The most important part of the data scattering corresponds to the first regime. Fig. 4.7 does not show data corresponding to the third regime. Similarly, the data in Fig. can be replotted as a function of a/d , where the same general trend is observed and where all the regimes are represented. The results of Ahmad et al. [43] imply that Tf decreases with the vibration amplitude, but they did not notice the scaling role of the amplitude, neither of the dimensionless amplitude a/d .

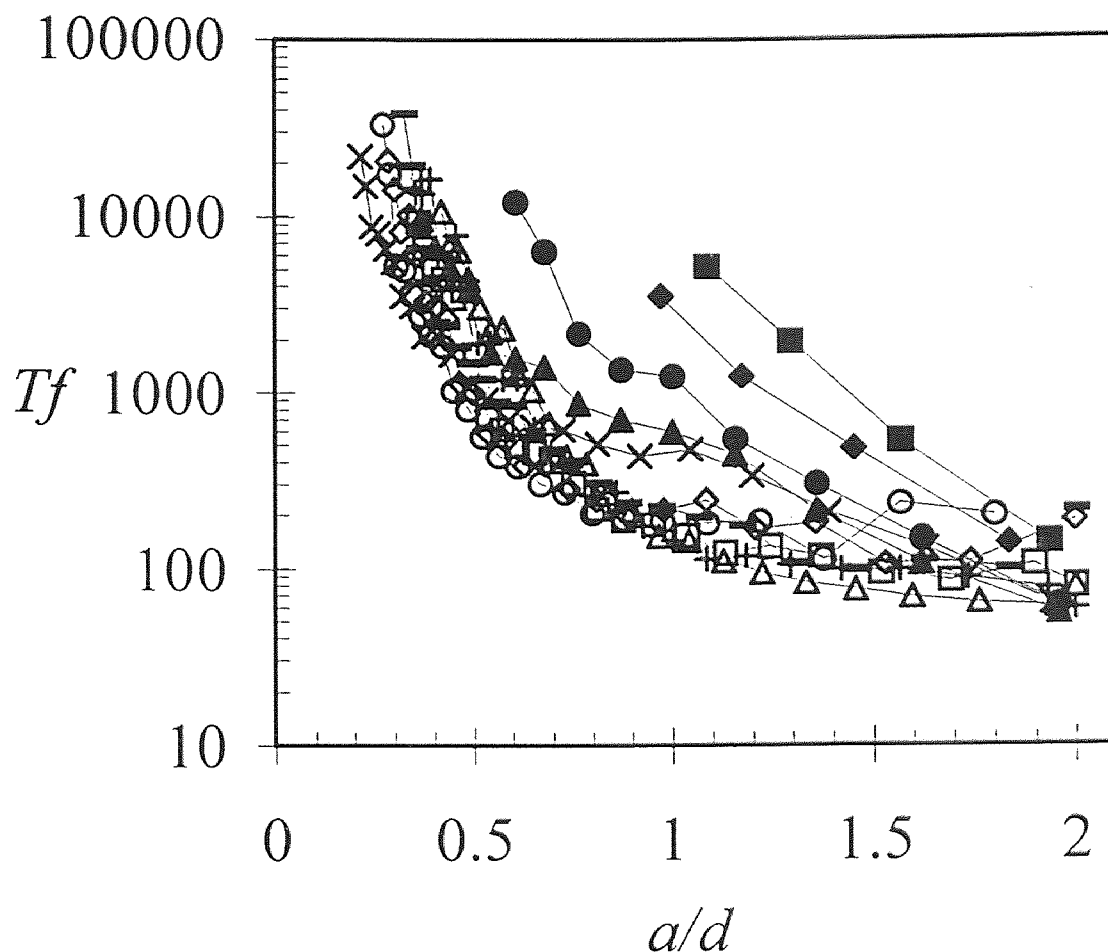


Figure 4.7. Dimensionless rise time Tf as a function of dimensionless amplitude a/d , for a range of relative acceleration Γ : (\blacklozenge) = 1.5, (\blacksquare) = 2, (\bullet) = 2.5, (\blacktriangle) = 3, (\times) = 3.5, (\circ) = 4.5, (\diamond) = 5, (\blacksquare) = 6, (\square) = 7, ($+$) = 8, (\triangle) = 9.

The idea that a/d is a good control parameter is discussed now. The objective is to characterize the rapid increase of Tf when a/d is decreased. Ahmad et al. placed a large sphere in a vibrated bed of sand having a mean diameter $d_A = 0.5$ mm (the subscript A refers to Ahmad) contained within a cylinder of 20.32 cm in diameter. The bed aspect ratio was $H/D_{\text{cyl}} = 0.625$ (similar to $H/D_{\text{cyl}} = 0.44$, which has been defined in Chapter 3). From Ahmad's results, one can try to compute the a/d_A values at which there is an increase of about an order of magnitude in T , from where T varies slowly with f (see Fig. 4

in Ref. [43]). This gives us a measure of the change in the rise behavior caused by the decrease of vibration amplitude. For a range of Γ values between 4 and 10, the values obtained are very consistent and have a mean of $a/d_A \cong 0.37 \pm 0.08$. It is already striking that, while there is more than a factor two between the smallest and largest value of Γ , the distribution width of a/d_A values is only 20% around the mean value. By following the same procedure with data of Fig. 4.7, it was found that $a/d \cong 0.4 \pm 0.1$. Since comparable values of a/d are obtained, it seems that the value of the amplitude alone is not enough to describe the response of the system but that it is a/d which correctly characterizes the divergence of T towards the small amplitude. Another striking result is that the frequencies corresponding to the computed a/d values are completely different in the two experiments. In fact, it can be shown that they depend on the diameter of the bed particles. First, it is clear that the vibration state is well defined by the values of a/d and Γ . Then, it is assumed that the experiments of Ahmad and ours are comparable and even equivalent if the values of a/d and of Γ are the same in both experiments. Consequently, there is a relationship between the frequencies and the ratio of bed particle diameters given by, $(f/f_A) = \sqrt{d_A/d}$. A substitution of the numerical values of the diameter leads to $f_A \cong 2.5f$, which agrees reasonably well with the actual scaling between the two systems. This last result enforces the idea that the amplitude must be scaled by the diameter of the bed particles. The validity of the previous analysis relies on the hypothesis that disparities in particle properties or in geometry can be neglected, as well as the additional effect of shearing at the walls caused by the motion of the piston.

4.4 More Observations on the Role Played by the Relative Acceleration

The rise time curves of fixed relative acceleration have particularly interesting properties. On these curves, there is a monotonous variation of Tf with frequency, and when Γ is varied, they are deformed regularly, in a continuous fashion. It was impossible to meet both of these properties when curves of fixed amplitude or velocity were plotted. It gives obviously a special status to the relative acceleration Γ . It is not so much a surprise since most of the other experimental and theoretical works described Γ as a control parameter.

However, it appears that the meaning of Γ is not as simple, since the rise time can be very different with the same relative acceleration. The role of the non-dimensional amplitude a/d has been put forward, as well as the importance of frequency as a transition parameter, but it makes the role of Γ more confusing. This section will describe what is the effect of Γ when either the frequency or amplitude is fixed. The case of high Γ is also addressed.

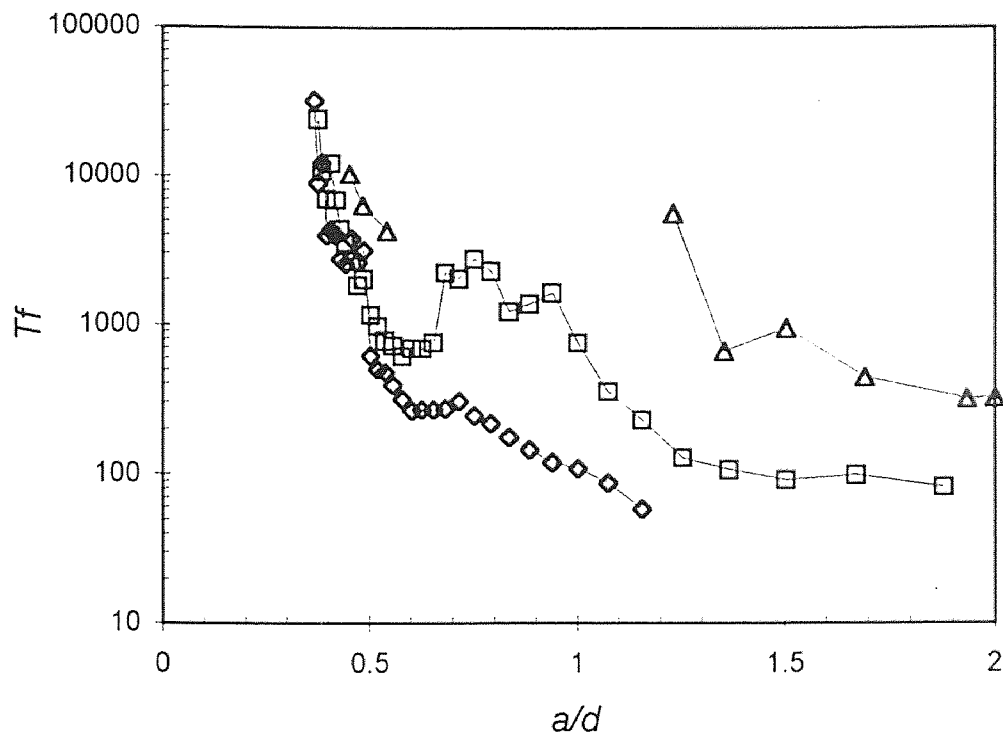


Figure 4.8. Dimensionless rise time Tf as a function of dimensionless vibration amplitude a/d for three different vibration velocity $a\omega$: (Δ) = 0.27 ms^{-1} , (\square) = 0.3 ms^{-1} , (\diamond) = 0.5 ms^{-1} . Note the irregularity of the constant velocity curves.

4.4.1 Rise Time at Fixed Frequency as a Function of Relative Acceleration

When the frequency is fixed, the rise time decreases with an increase of relative acceleration as can be deduced from Fig. 4.3 or Fig. 4.5. It is equivalent to say the rise time decreases with an increase of amplitude. However, it is not an obvious result. In section 4.3, Γ is kept fixed while here f is kept fixed. This result seems to suggest that the rise time will always decrease with an increase in amplitude whatever is the fixed parameter. It is true when frequency, or acceleration is fixed, but not when velocity is fixed as shown on Fig. 4.8. Alternatively, the rise time will always decrease with an increase in relative acceleration at fixed frequency, but not at fixed amplitude as described in the following section.

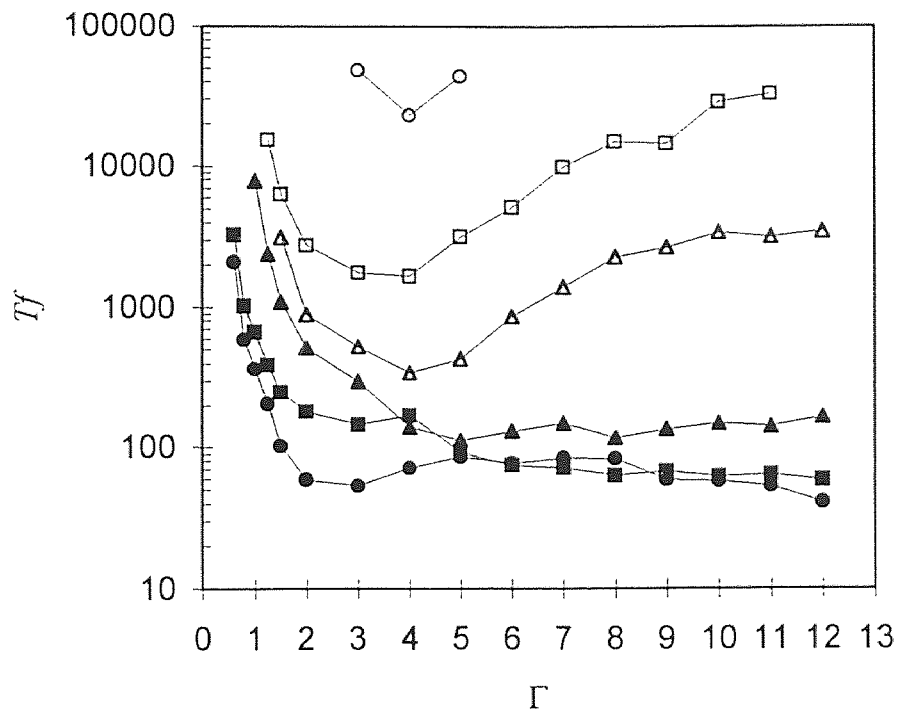


Figure 4.9. Dimensionless rise time T_f as a function of relative acceleration Γ for a range of fixed dimensionless vibration amplitude a/d : (\circ) = 0.1, (\square) = 0.25, (\triangle) = 0.5, (\blacktriangle) = 1, (\blacksquare) = 1.5, (\bullet) = 2.

4.4.2 Rise Time at Fixed Amplitude as a Function of Relative Acceleration

When the amplitude is fixed, the rise time variation with relative acceleration appears as in Fig. 4.9. For $a/d \geq 1$, Tf decreases with Γ , but when $a/d < 1$ and $\Gamma > 4$, Tf increases with Γ . No clear explanation has been found to account for this strange behavior. However, it appears that this irregularity is a consequence of the heaping-non-heaping transition. Indeed, in Fig. 4.9, the condition to observe the irregularity is:

$$a/d < 1 \text{ and } \Gamma > 4, \text{ or } a/d < 1 \text{ and } f > \frac{1}{\pi} \frac{\sqrt{g/d}}{\sqrt{a/d}}.$$

A necessary condition is thus that $a/d < 1$ and $f > f_{min}$ where $f_{min} = \frac{1}{\pi} \sqrt{g/d} = 17.7 \text{ Hz}$.

Interestingly, the irregular behavior appears only when there is no heaping. In Fig. 4.8, the jump observed in the curves of fixed velocity has the same origin. When $a\omega = 0.3 \text{ ms}^{-1}$, the irregularity occurs for $a/d \cong 0.7$, and it corresponds also to a value of the relative acceleration $\Gamma \cong 4.1$.

4.4.3 “Inverse” Convection at High Acceleration

When $\Gamma > 13$, a new regime with an inverse convection pattern is observed. The large ball will not rise, but instead will sink when it is placed at the center of the top surface. In this regime, an upward flow occurs at the walls while a downward flow shows up towards the center of the container. This new behavior is concomitant with a subharmonic bifurcation of the bed response. Two distinct parts of the bed are delimited along a line corresponding to a diameter of the cylinder, and oscillate out of phase with a defect connecting them. This behavior is reminiscent of the subharmonic response of a vibrated bed observed by Douady et al. [24].

At the defect location, the opposite motion of the two parts of the bed creates a shearing much bigger than the single motion of one part of the bed relative to the walls. Thus, the downward flow occurs where the shearing is maximum. It is a very interesting conclusion since it helps to understand the usual convection pattern where the downward flow appears at the walls. Indeed, when the whole bed layer oscillates in phase, the walls are the major source of shearing and the shearing effect will decay towards the bed center.

Then, it is logical to observe a downward flow at the walls where the shearing is maximum. The remaining question is why ?

CHAPTER 5

RESULTS: TRACKING THE MOTION OF THE LARGE SPHERE

These results are the first application of the tracking technique to an experimental investigation. A panorama of the possible trajectories is presented. It is followed by a description of the three-dimensional motion where is shown the main effect of the initial radial coordinate of the ball. At last, the problems encountered and possible developments are discussed.

5.1 Phenomenology of Trajectories

In this section, only the vertical displacement is considered. Various shapes of trajectories have been observed. The ball is seen rising up, sinking down, moving up and down and its motion shows period doubling depending on the vibration parameters but also the height of the granular layer. This diversity is partly due to the diversity of macroscopic behaviors displayed by a granular bed.

With the experimental setup used, heaping can be observed either for $\Gamma < 1$ or $\Gamma > 1$. When $\Gamma = 1.29$ and for $f = 7.5$ Hz, the trajectory of the ball is composed of single flights with a rise mostly linear with time, except at the very beginning and at the very end of the rise (see Fig. 5.1). After reaching the top of the heap, the ball falls along the slope towards the walls and its altitude dwindles as seen on Fig. 5.1. Another trajectory is shown for $\Gamma = 2.06$ and $f = 12$ Hz in Fig. 5.2. The first part of the trajectory, before the ball starts to rise, is very similar to the previous case, simply because it corresponds to the establishment of the permanent vibration regime. The last part of the trajectory in Fig. 5.2 is qualitatively different. The ball slows down earlier and it results in a more pronounced curvature of the trajectory. In addition, the rise time is slower in this case, even though the relative acceleration is bigger. It is due to the fact that the amplitude is smaller in Fig. 5.2 ($a/d = 1.12$) than in Fig. 5.1 ($a/d = 1.8$). Thus, it seems that the amplitude has an effect on the shape of the ball trajectory, especially far from the vibration source.

When $f > 15$ Hz, it has been explained in Chapter 4 that a convective regime without heaping is observed. Fig. 5.3 shows the trajectory of the ball in this regime when

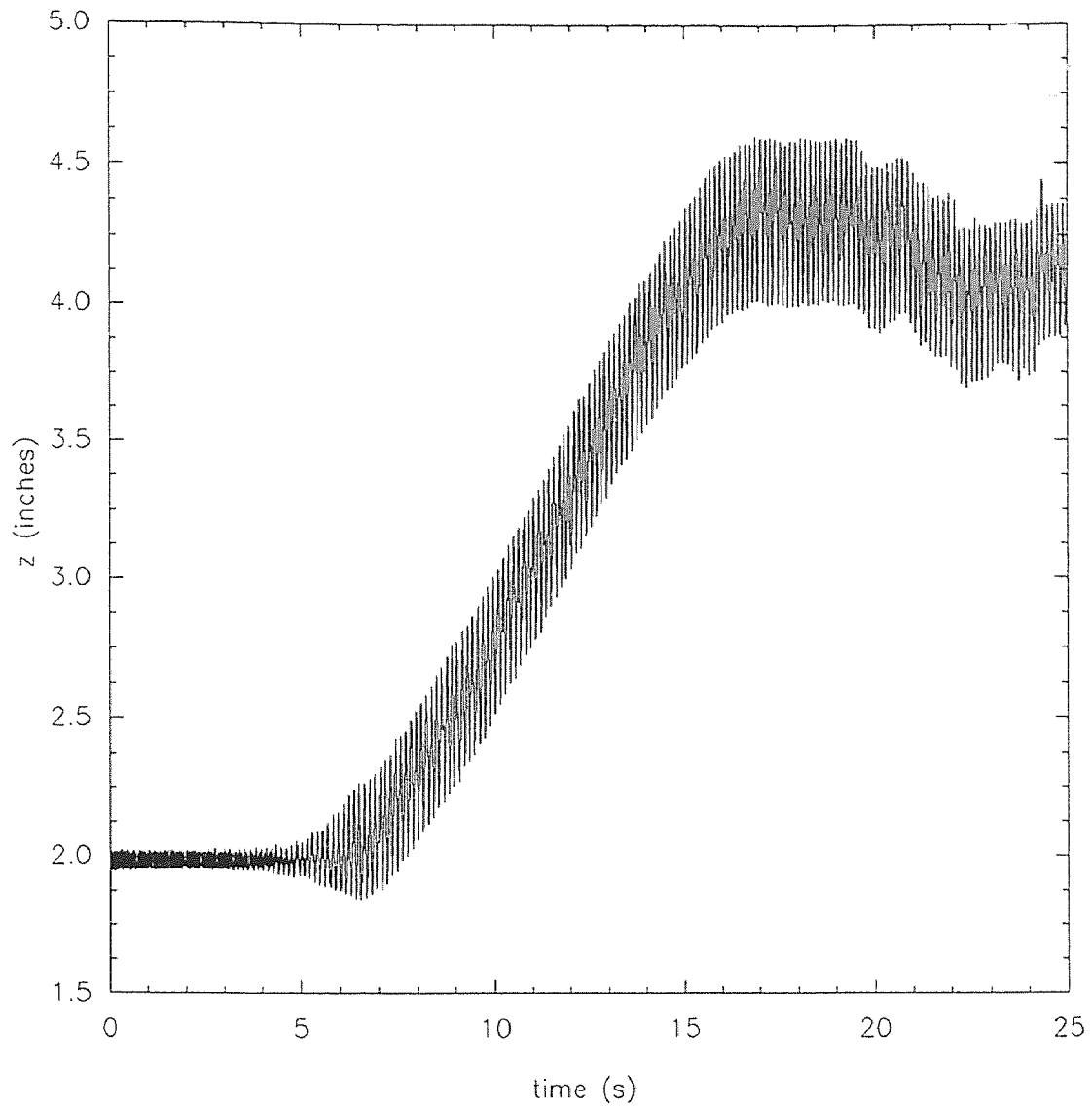


Figure 5.1. Plot of the vertical position z as a function of time, in the case of heaping at large amplitude ($a/d=1.8$) and $f=7.5$ Hz.

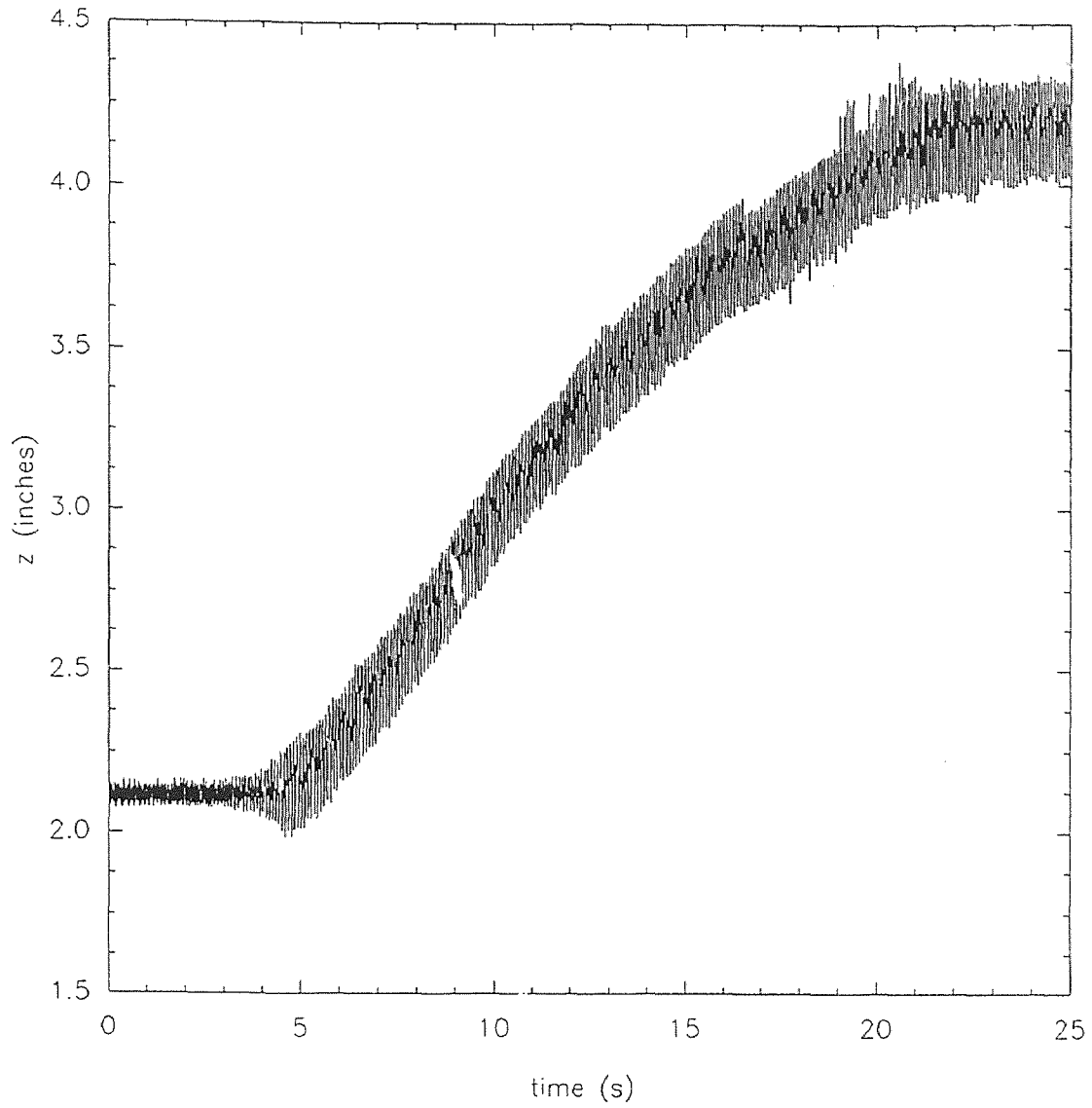


Figure 5.2. Plot of the vertical position z as a function of time, in the case of heaping at small amplitude ($a/d=1.12$) and $f=12$ Hz.

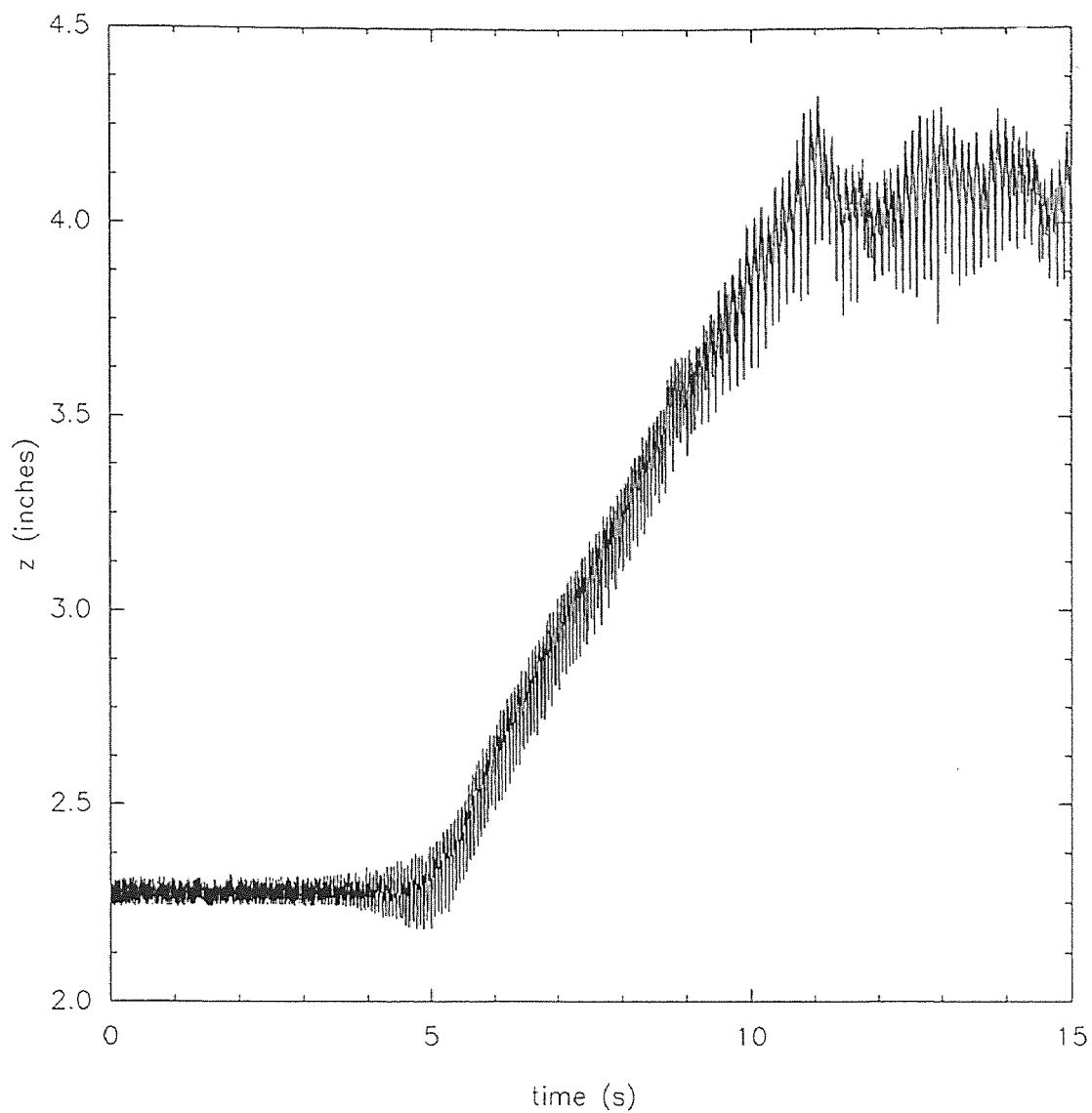


Figure 5.3. Plot of the vertical position z as a function of time, in the case of convection without heaping at high amplitude ($a/d=1.8$) and $f=18$ Hz. Period doubling is observed clearly above $z \cong 3.5$ ''.

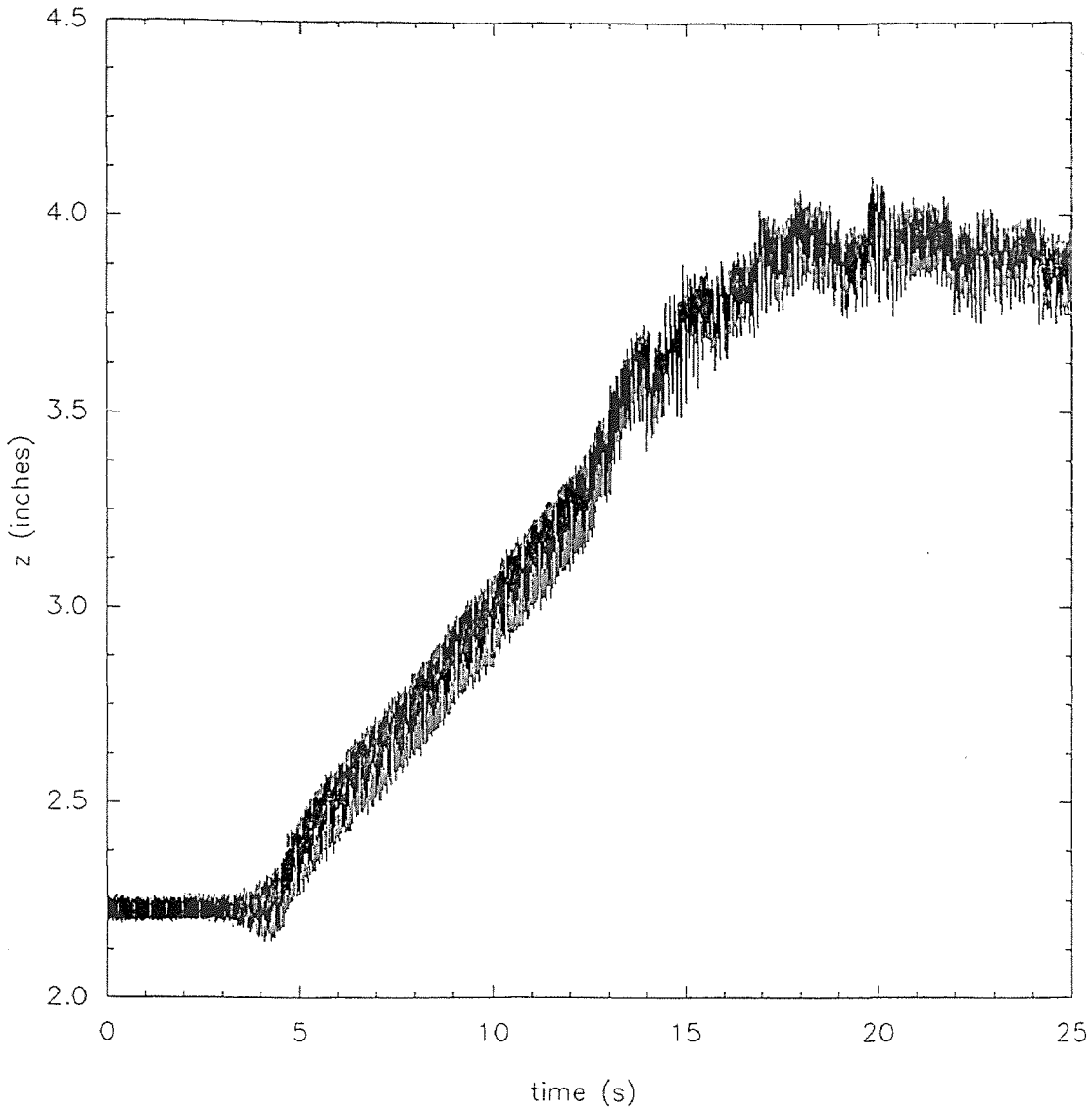


Figure 5.4. Plot of the vertical position z as a function of time, in the case of convection without heaping at small amplitude ($a/d = 1.12$) and $f = 18$ Hz. There is almost no period doubling.

$\Gamma = 7.45$ and $f = 18$ Hz. Again, the average trajectory is highly linear with time. The motion is initially composed of single flights, but before reaching the surface a period doubling of the motion occurs. Period doubling is characteristic of a non-linear and dissipative system and is consequently strongly dependent on the dissipative properties of the medium. When a granular layer is fluidized, the upper part of the layer is less dense than the bottom, and the energy dissipation will be more important in a dense region, due to the greater probability of collisions. Furthermore, for given control parameters, period doubling will occur preferentially where the dissipation is smaller. It is probably what happens in Fig. 5.3. When $f = 18$ Hz and $\Gamma = 4.64$, the trajectory observed is as shown in Fig. 5.4. Mainly the same observations can be made than in the previous case. However, the period doubling is much less important and the trajectory displays a more pronounced curvature when the ball approaches the top surface. The different amplitudes, $a/d = 1.8$ in the first case and $a/d = 1.12$ in the second, are responsible for the change in shape, like already shown for heaping trajectories, but are also responsible for the different period doubling behavior. Indeed, a smaller amplitude will result in a denser upper layer, which increases the dissipative properties of the medium, and thus, will not facilitate period doubling.

In some cases, an inverse convection is observed. It seems to occur only for high acceleration. Fig. 5.5 shows the trajectory of the ball sinking to the bottom of the container, when $f = 27$ Hz and $\Gamma = 16.7$ ($a/d = 1.8$). In first approximation, the average trajectory looks linear. The details of the ball motion shows that the motion is composed of irregular flights. An analysis by Fourier transform of the trajectory gives a very noisy spectrum with three dominant frequencies at f , $f/2$ and $f/4$ (see Fig. 5.9). Fig. 5.6 shows another trajectory for $f = 27$ Hz and $\Gamma = 10.4$ ($a/d = 1.12$). The ball sinks more slowly, and the trajectory is slightly curved at the top. Again, the amplitude seems responsible for the more pronounced curvature of the trajectory. In addition, the downward motion of the ball is dominated only by the vibration frequency f , as shown by the Fourier analysis in Fig. 5.10.

A few trajectories correspond to a motion similar to the “whale” effect described in Chapter 2. The ball goes up and down, but unlike in the “whale” effect, the ball never

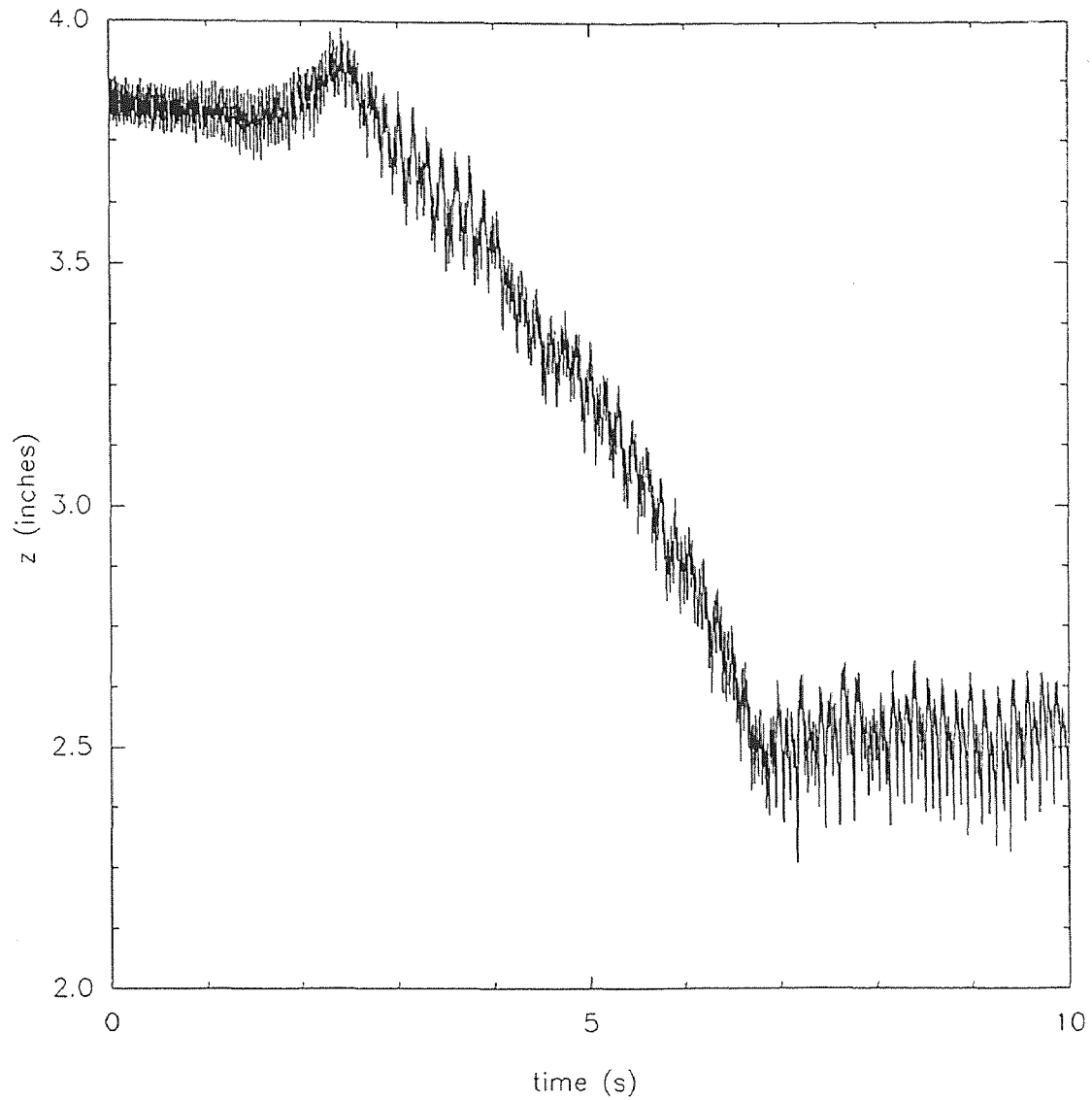


Figure 5.5. Plot of the vertical position z as a function of time, in the case of inverse convection at large amplitude ($a/d = 1.8$) and $f = 27$ Hz. Fourier analysis shows that the oscillatory motion is dominated by three frequencies : $f, f/2, f/4$.

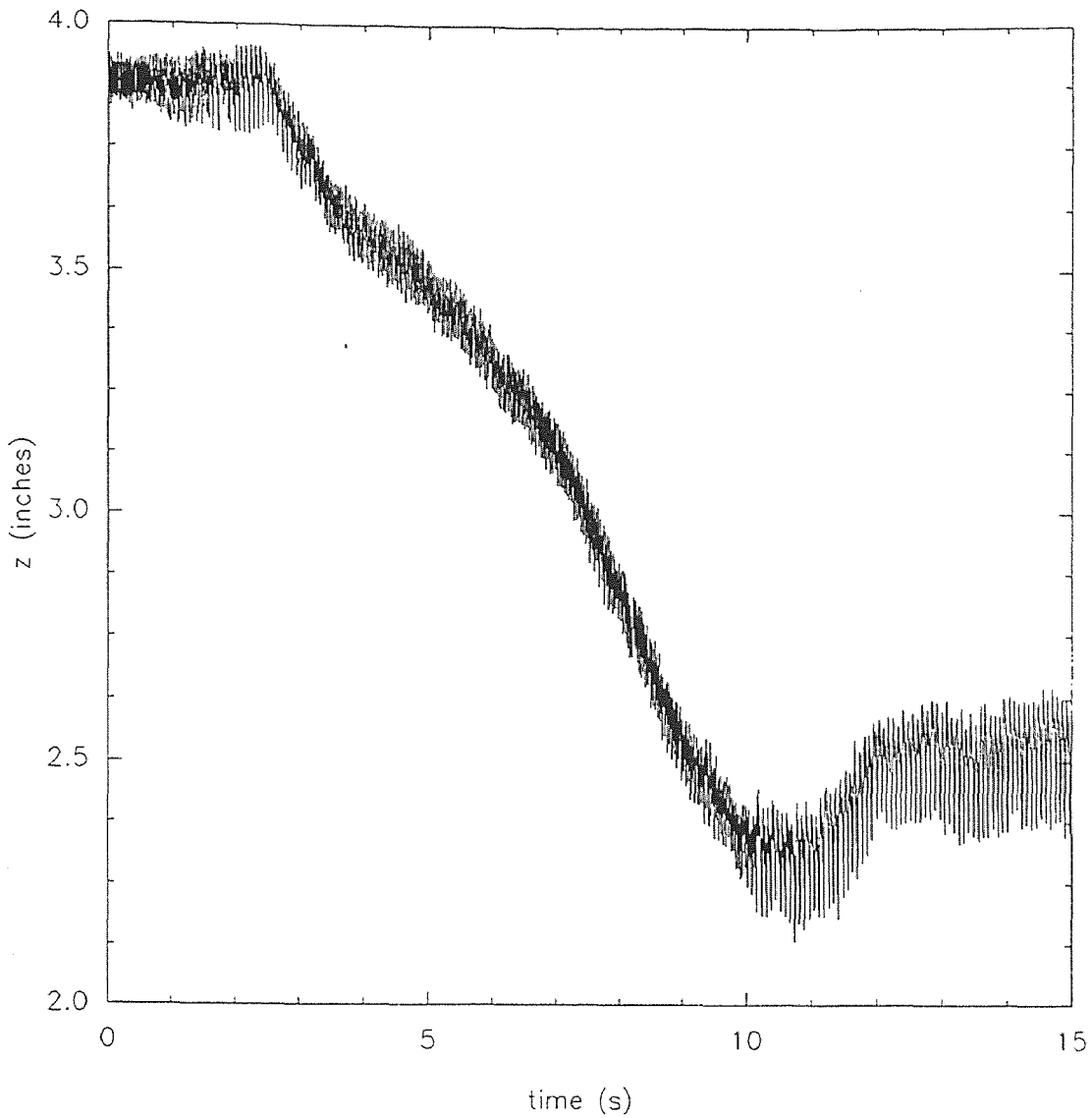


Figure 5.6. Plot of the vertical position z as a function of time, in the case of inverse convection at small amplitude ($a/d = 1.12$) and $f = 27$ Hz. Fourier analysis shows that the oscillatory motion is associated with only one frequency : f .

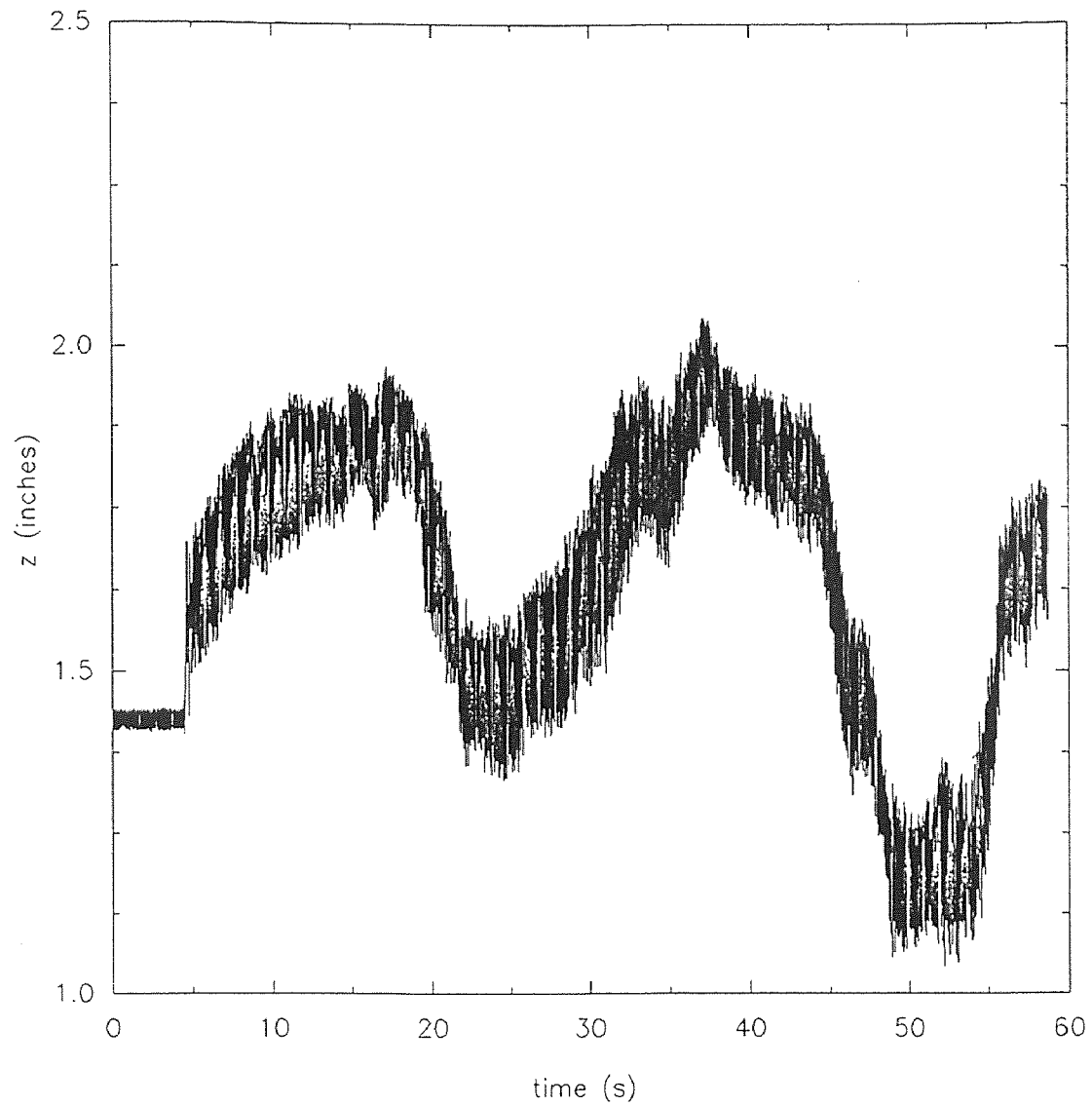


Figure 5.7. Plot of the vertical position z as a function of time for $a/d = 1$ and $f = 25$ Hz. The motion qualitatively corresponds to the "whale" effect.

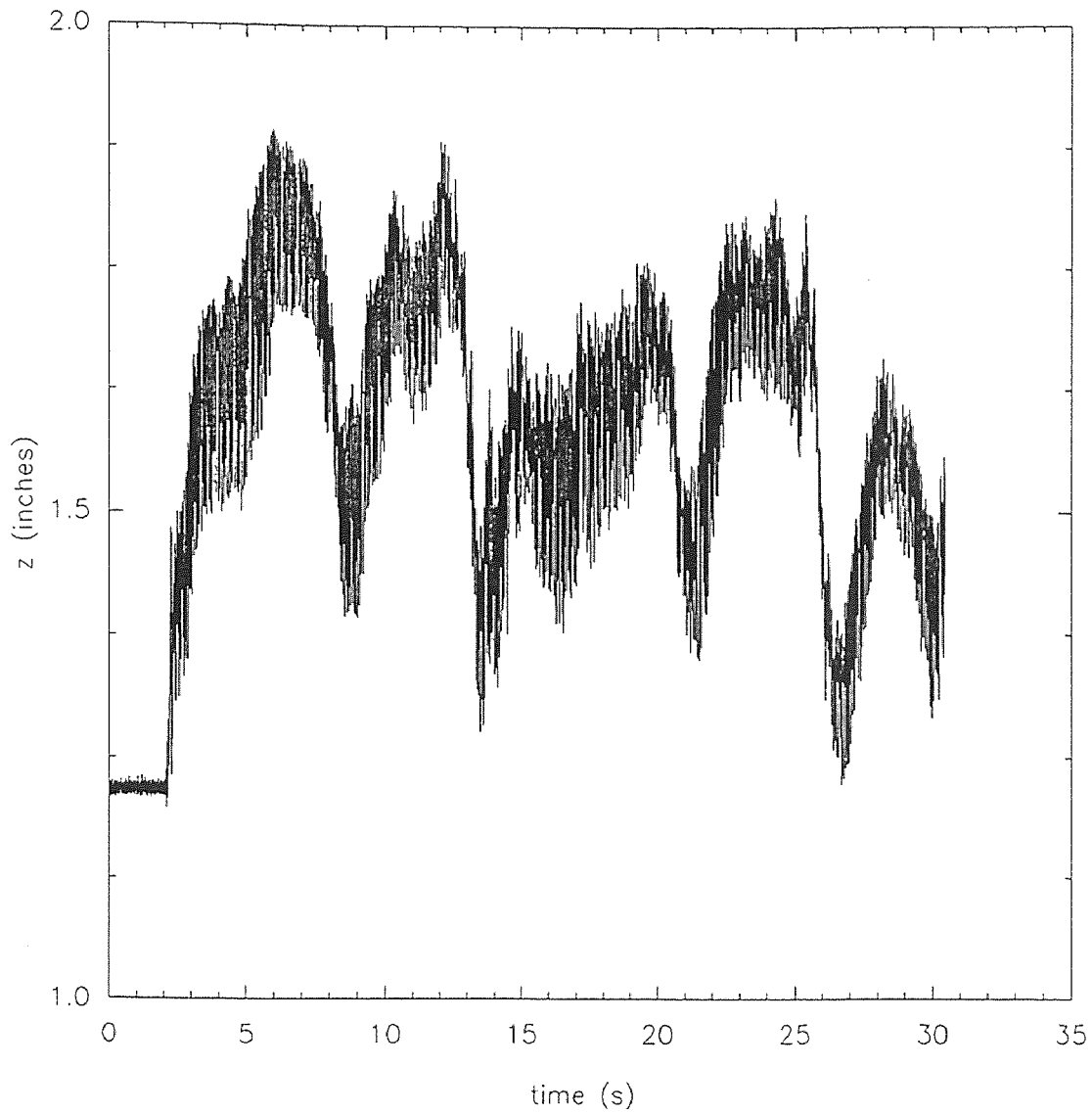


Figure 5.8. Plot of the vertical position z as a function of time for $a/d=1$ and $f=30$ Hz. The motion qualitatively corresponds to the "whale" effect.

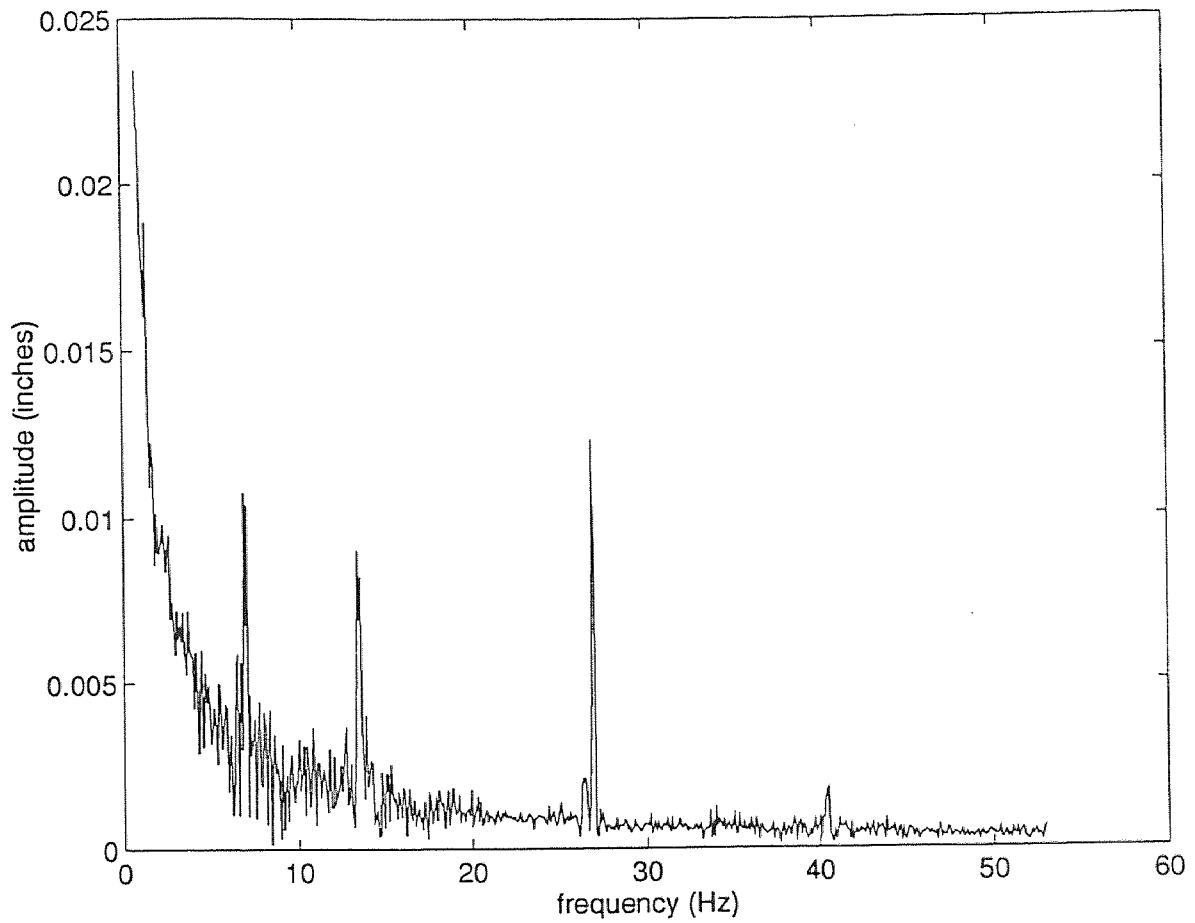


Figure 5.9. Amplitude spectrum corresponding to the trajectory of Fig. 5.5. There are three dominant frequency in this spectrum, at f , $f/2$, $f/4$. The frequencies higher than the vibration frequency are not physically significant.

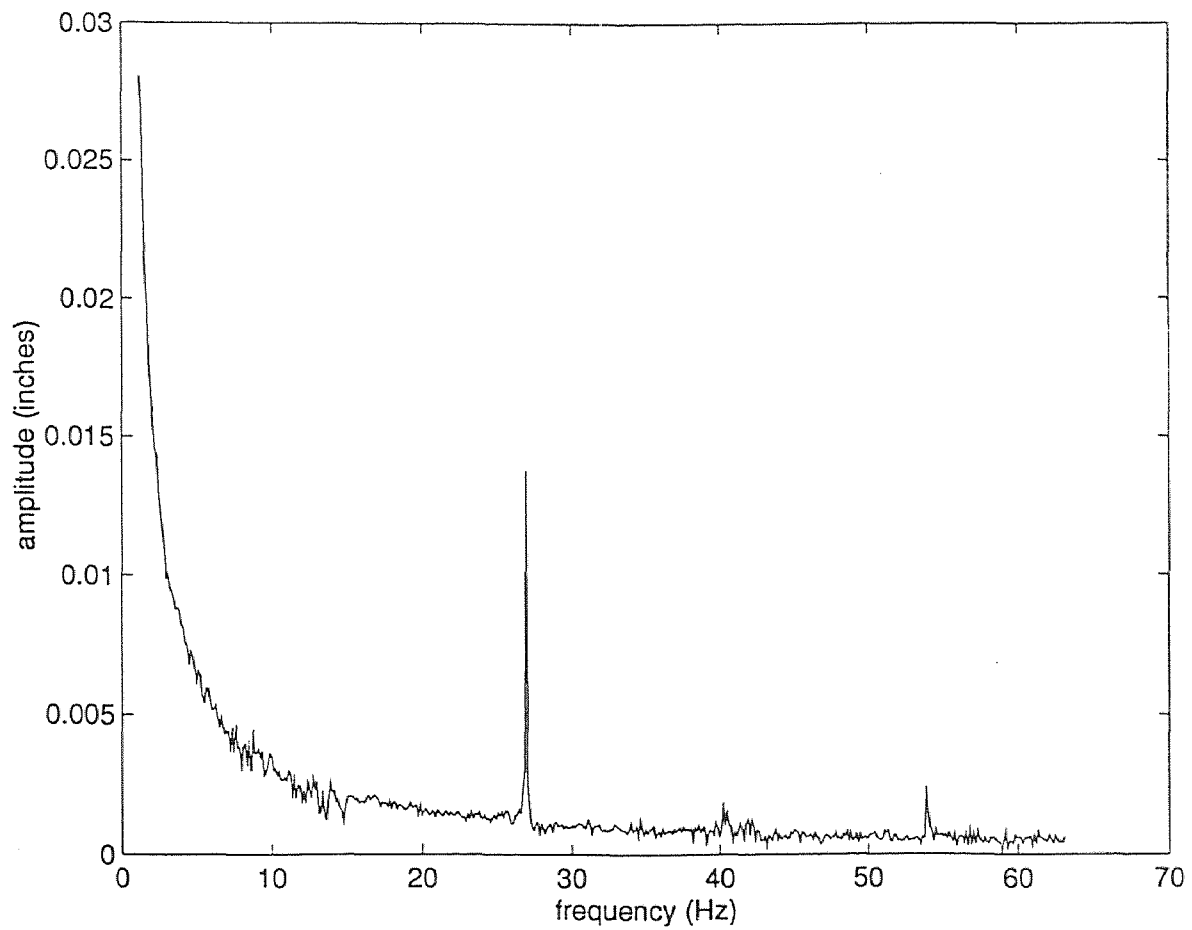


Figure 5.10. Amplitude spectrum corresponding to the trajectory in Fig. 5.6. There is only one dominant frequency in this spectrum, at $f = 27$ Hz. The frequencies higher than the vibration frequency are not physically significant.

reaches the surface and does not seem to follow a convection roll. Fig. 5.7 and Fig. 5.8 are two examples of this type of trajectory. In both cases, the amplitude of the oscillation is about 0.6 inches and the ball goes down more easily than it goes up. The physical meaning of these trajectories is very unclear. Moreover, it is difficult to predict what are the required conditions to observe them. In the present state of the experiment, the ball would rise to the top with the same vibration conditions than in Fig. 5.7 and Fig. 5.8.

5.2 Analysis of the Three-Dimensional Motion

The trajectories described in this section are obtained in a cylindrical coordinate system as shown in Fig. 5.11. The main displacement occurs in the vertical direction and the rotational motions are insignificant. The effect of the initial radial position is illustrated using two examples. The vibration amplitude used is $a/d = 1$ and the frequency $f = 15$ Hz.

In the first example, the ball is initially positioned at the center of the piston surface. The vertical coordinate z is plotted in Fig. 5.12, and the rise appears very regular and the oscillatory motion has a frequency $f/2$. In Fig. 5.13, the radial displacement r during the first 20 seconds (when the ball rises) is about one bed spheres diameter. Just before the ball reaches its maximum altitude, r increases significantly because the ball is moving towards the walls. There is also a curious periodic oscillation of the radial displacement at $f/2$, which can be seen on all the other coordinates. In Fig. 5.14, the angle θ varies very little, which means there almost no orthoradial motion. There are also rotational motions, but they appear small in comparison with a complete rotation of 360° , as shown in Fig. 5.15, 5.16 and 5.17.

In the second example, the ball is initially positioned on the piston surface, but is now touching the cylinder walls. The vertical motion z , shown in Fig. 5.18, is qualitatively similar to Fig. 5.12. All the rotations and the orthoradial displacement are very small. The only important difference is the radial displacement, shown in Fig. 5.19 : r goes down, reaches a minimum, and slightly increases at the end. In order to rise, the ball must avoid the downward flow along the walls. Consequently, the ball is pushed inside the bed while rising, and close to the surface, the ball start moving back towards the wall. The maximum distance from the walls reached by the ball surface is about $5d$. This value is bigger than

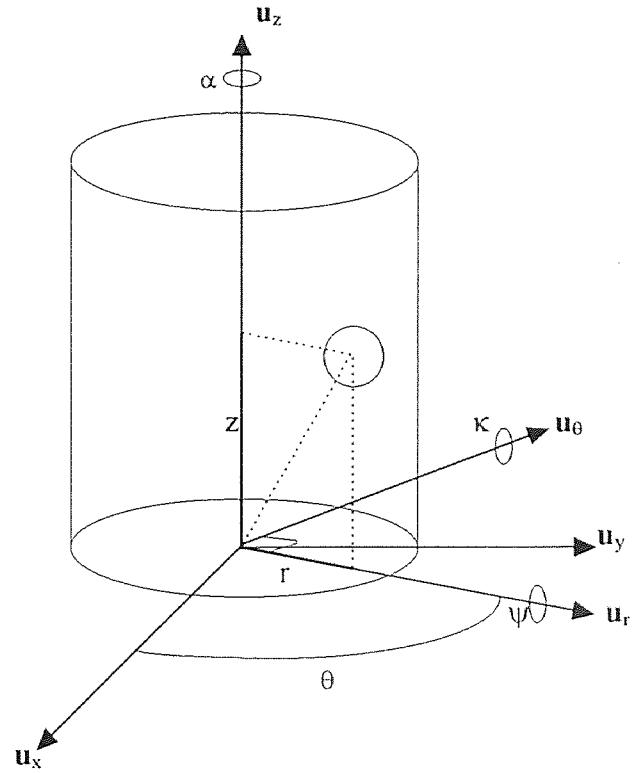


Figure 5.11. Position of the large ball (r, θ, z) in a cylindrical coordinate system $(\mathbf{u}_r, \mathbf{u}_\theta, \mathbf{u}_z)$. Alpha (α) is the rotation around \mathbf{u}_z . Psi (ψ) is the rotation around \mathbf{u}_r . Khi (κ) is the rotation around \mathbf{u}_θ .

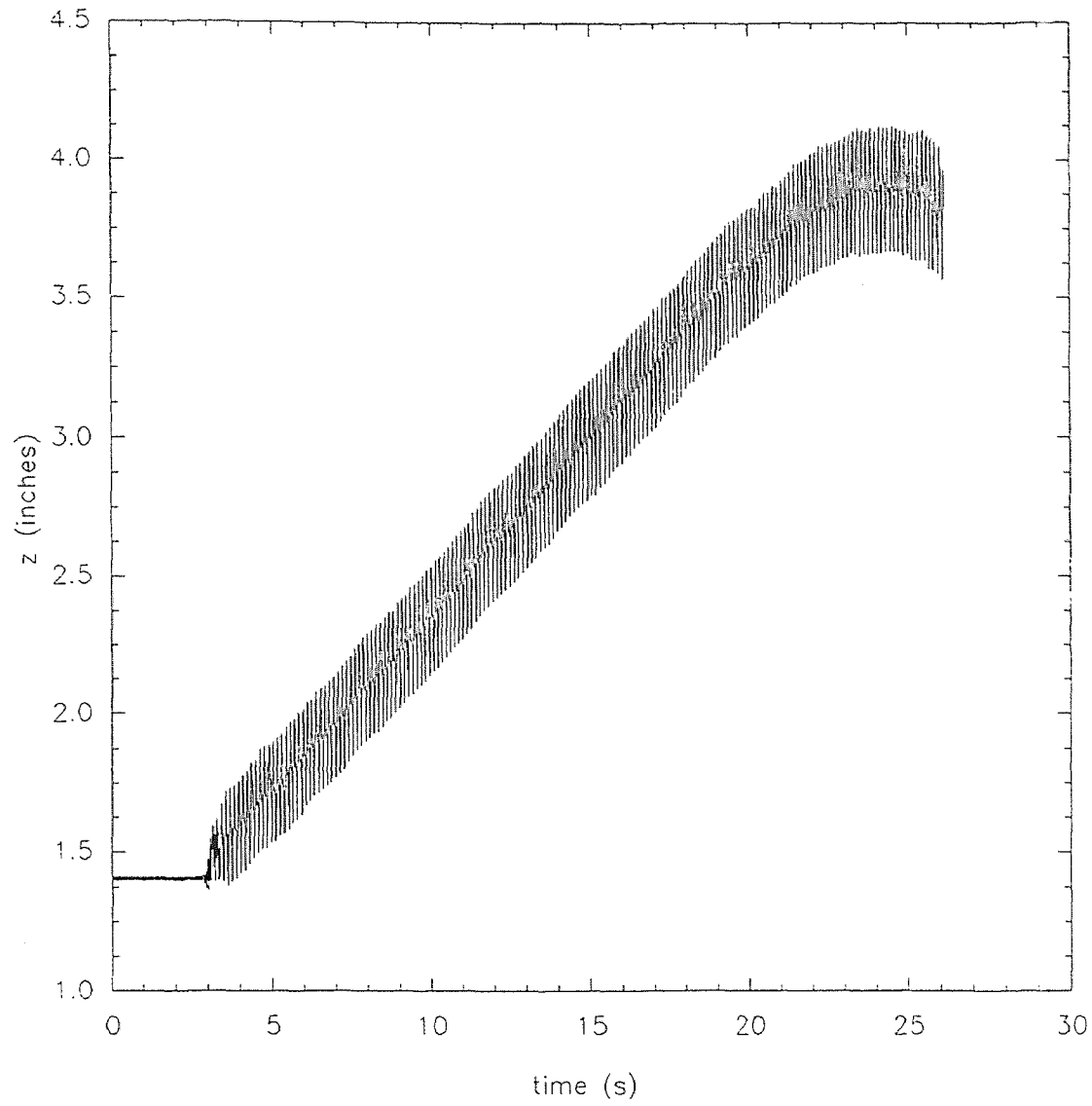


Figure 5.12. Plot of the vertical position z as a function of time for $a/d = 1$ and $f = 15$ Hz. Heaving is observed, the rise is linear with time, and the ball oscillates at $f/2$.

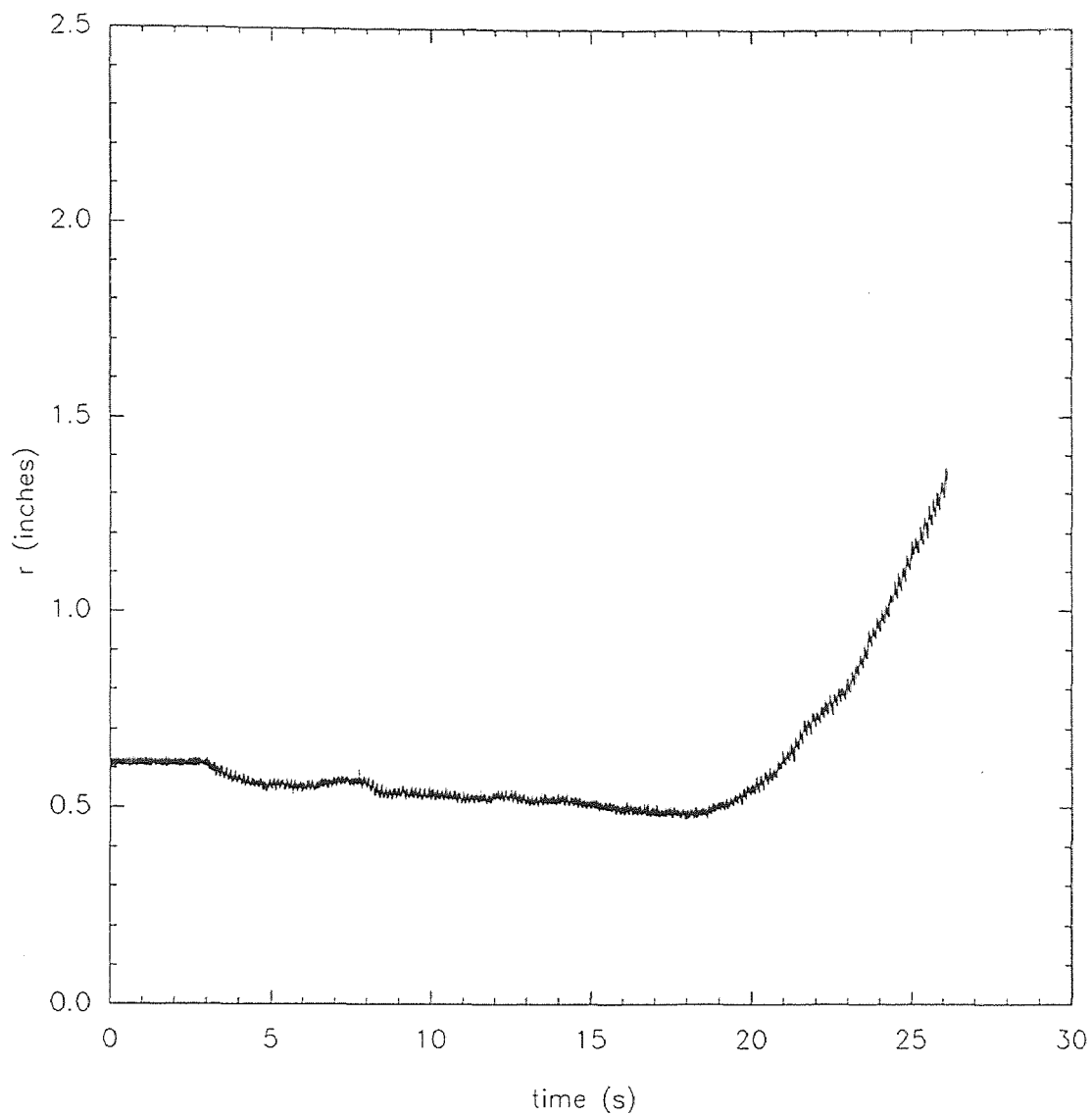


Figure 5.13. Plot of the radial displacement r as a function of time for $a/d = 1$ and $f = 15$ Hz. A residual oscillation at $f/2$ is observed.

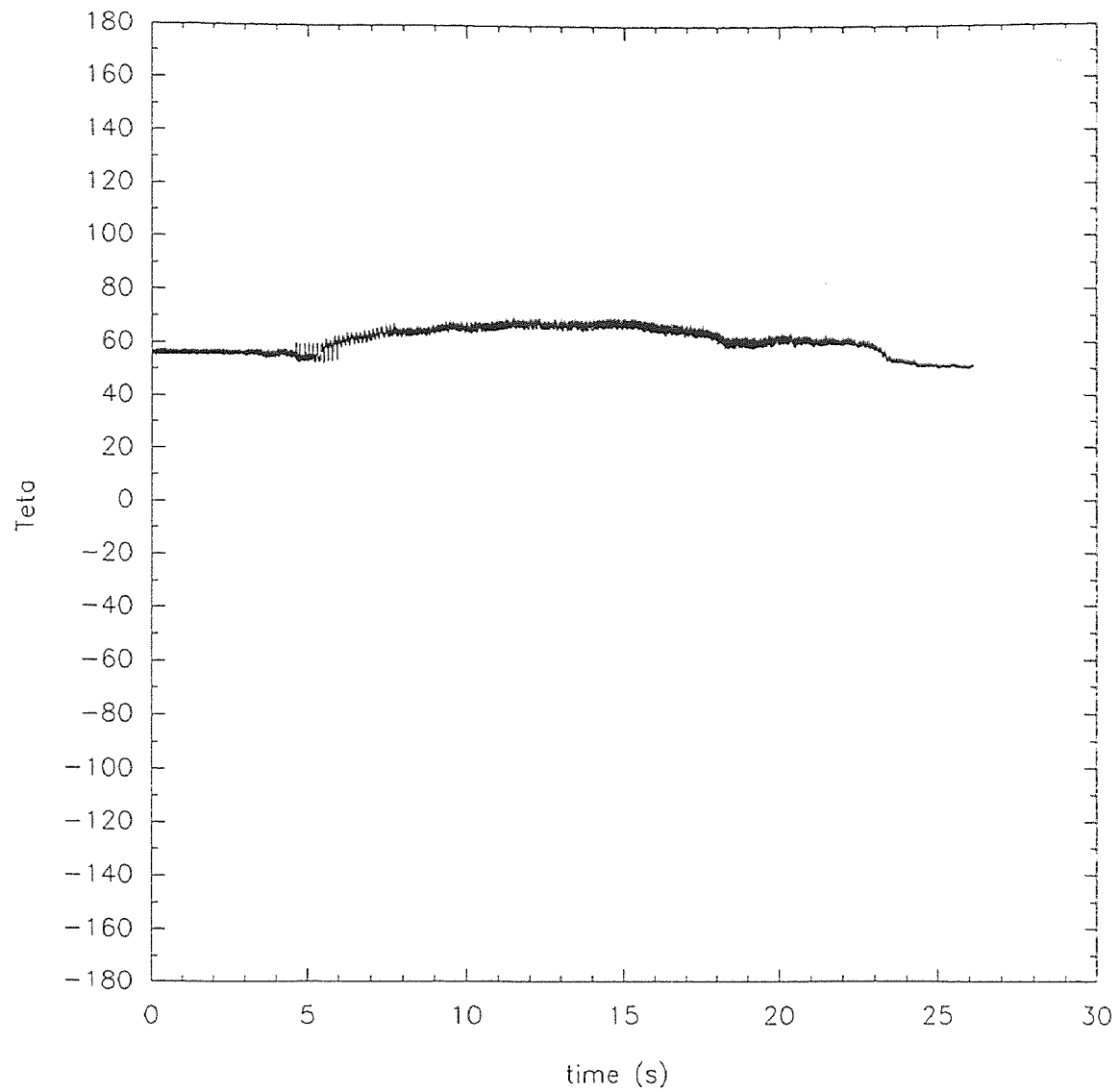


Figure 5.14. Plot of the angular motion Θ as a function of time, for $a/d = 1$ and $f = 15$ Hz. A residual oscillation at $f/2$ is observed.

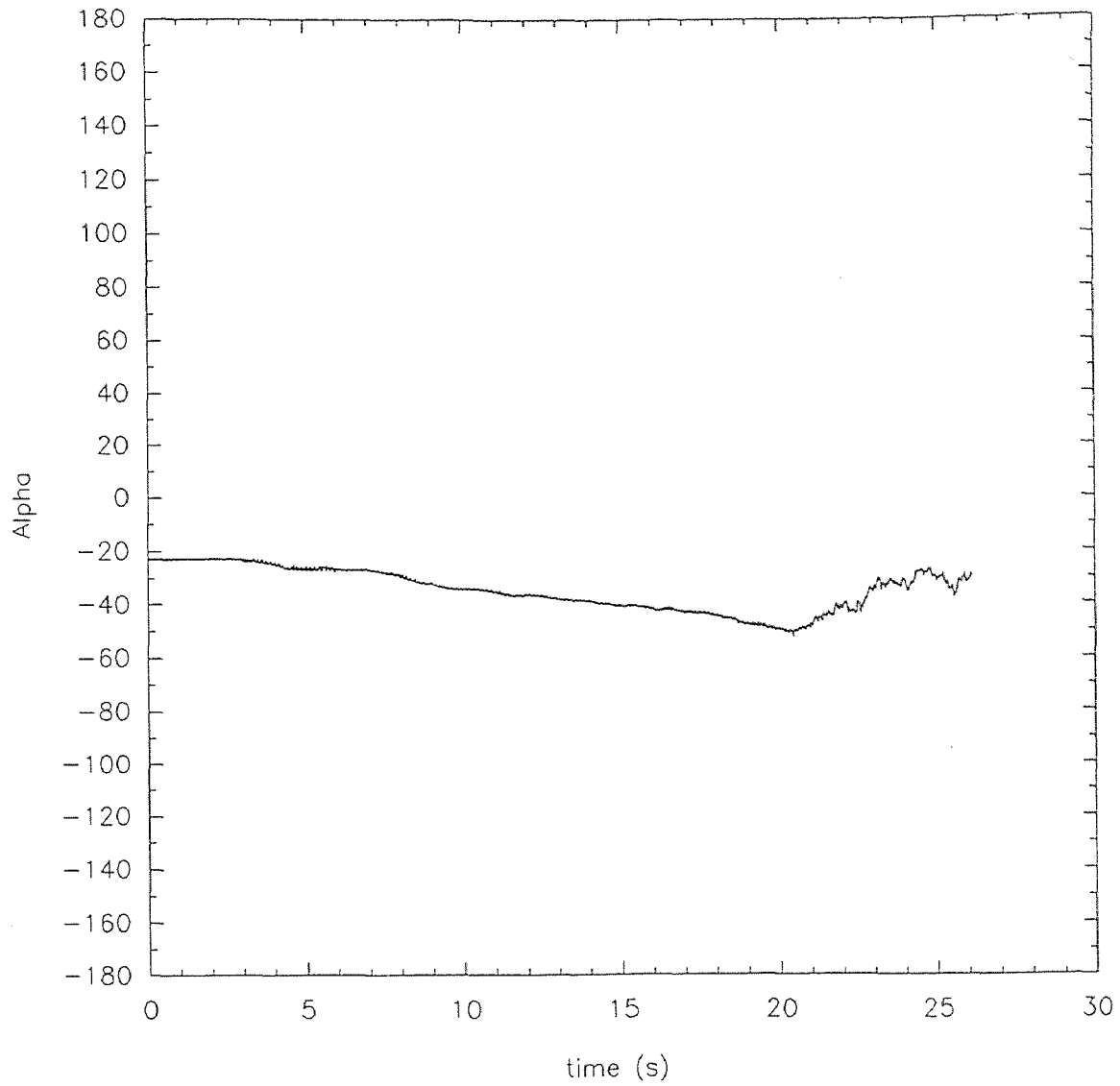


Figure 5.15. Plot of the rotational motion α as a function of time for $a/d = 1$ and $f = 15$ Hz. A residual oscillation at $f/2$ is observed.

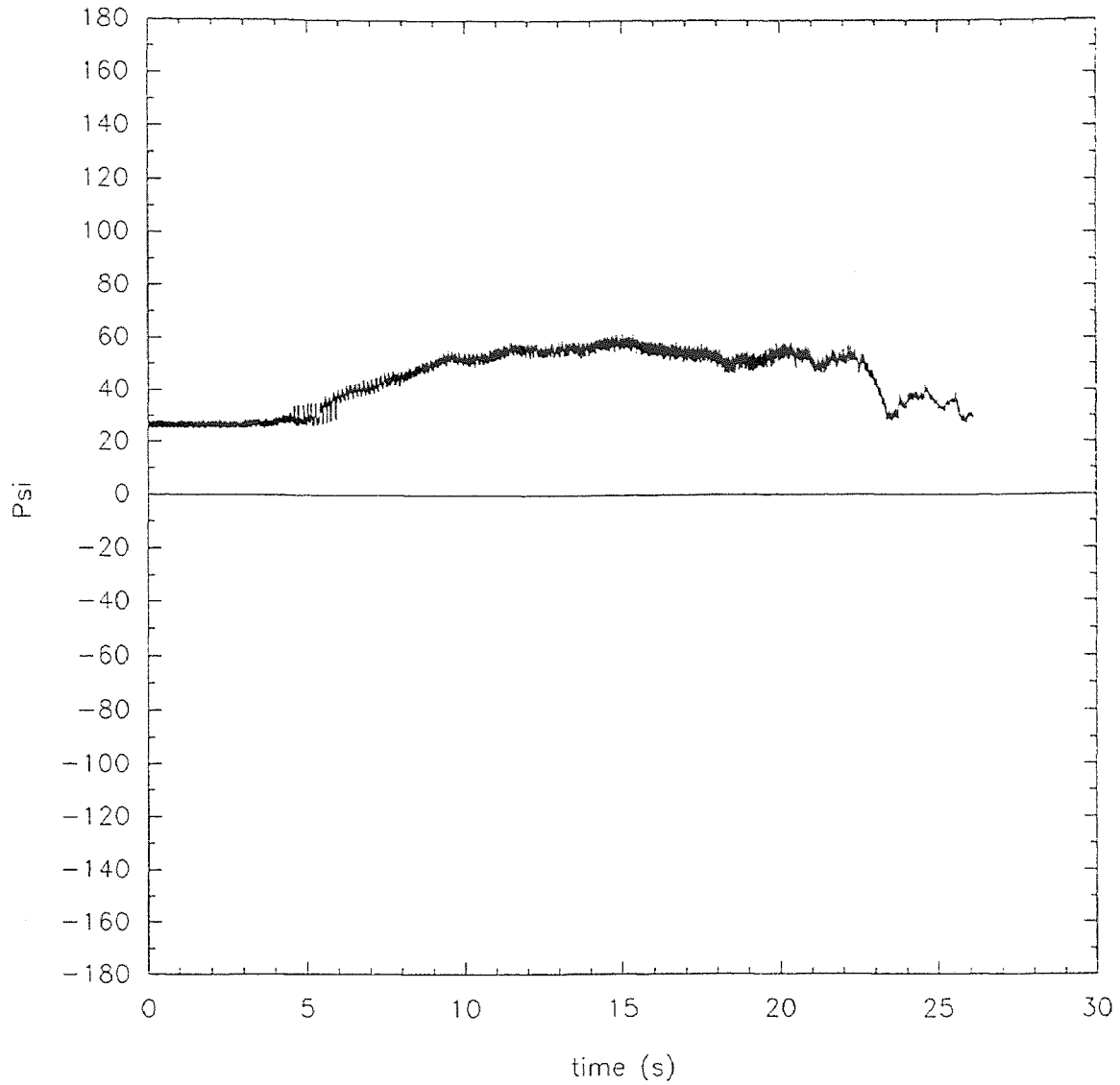


Figure 5.16. Plot of the rotational motion Ψ as a function of time for $a/d = 1$ and $f = 15$ Hz. A residual oscillation at $f/2$ is observed.

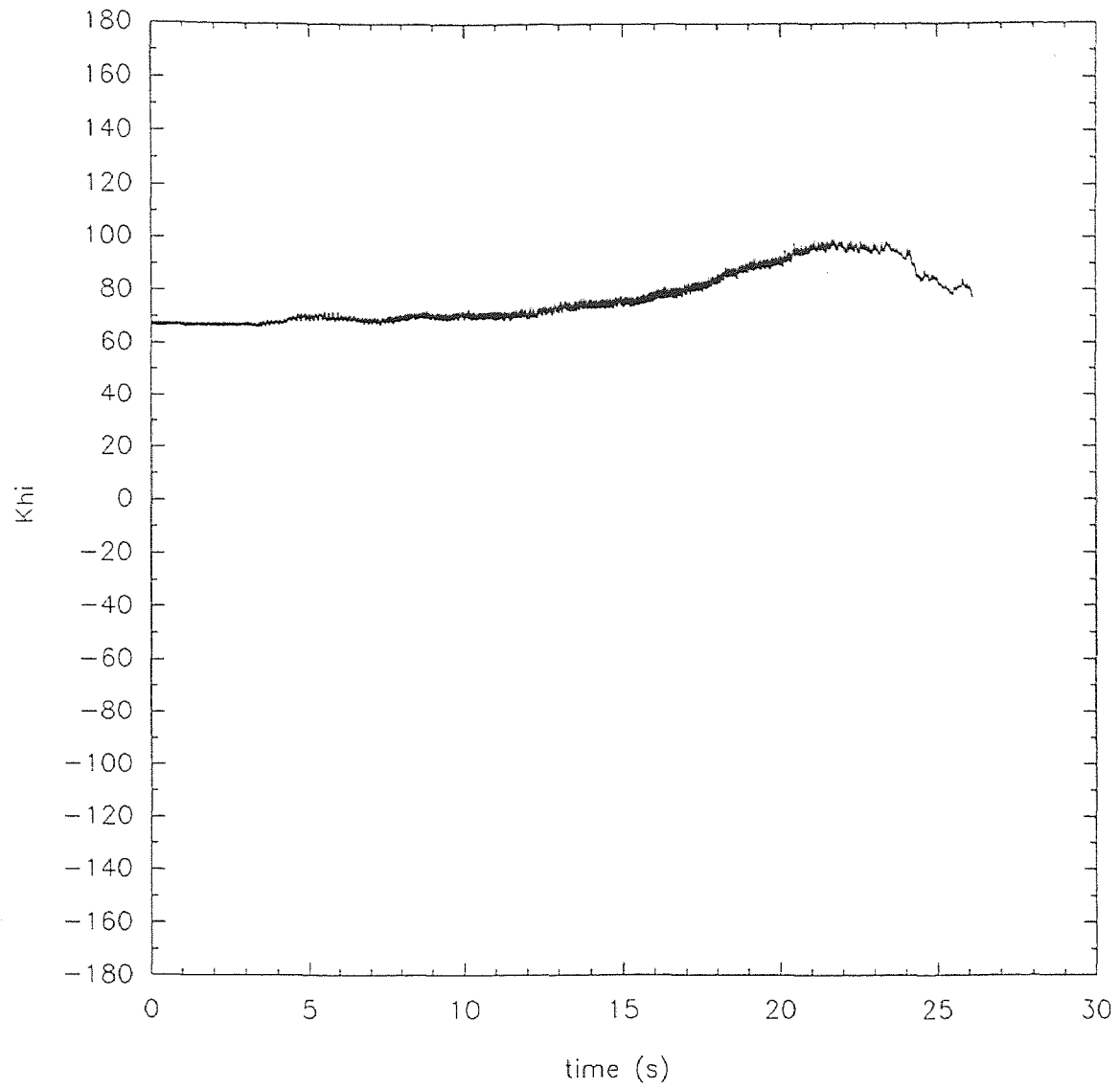


Figure 5.17. Plot of the rotational motion K_{hi} as a function of time for $a/d = 1$ and $f = 15$ Hz. A residual oscillation at $f/2$ is observed.

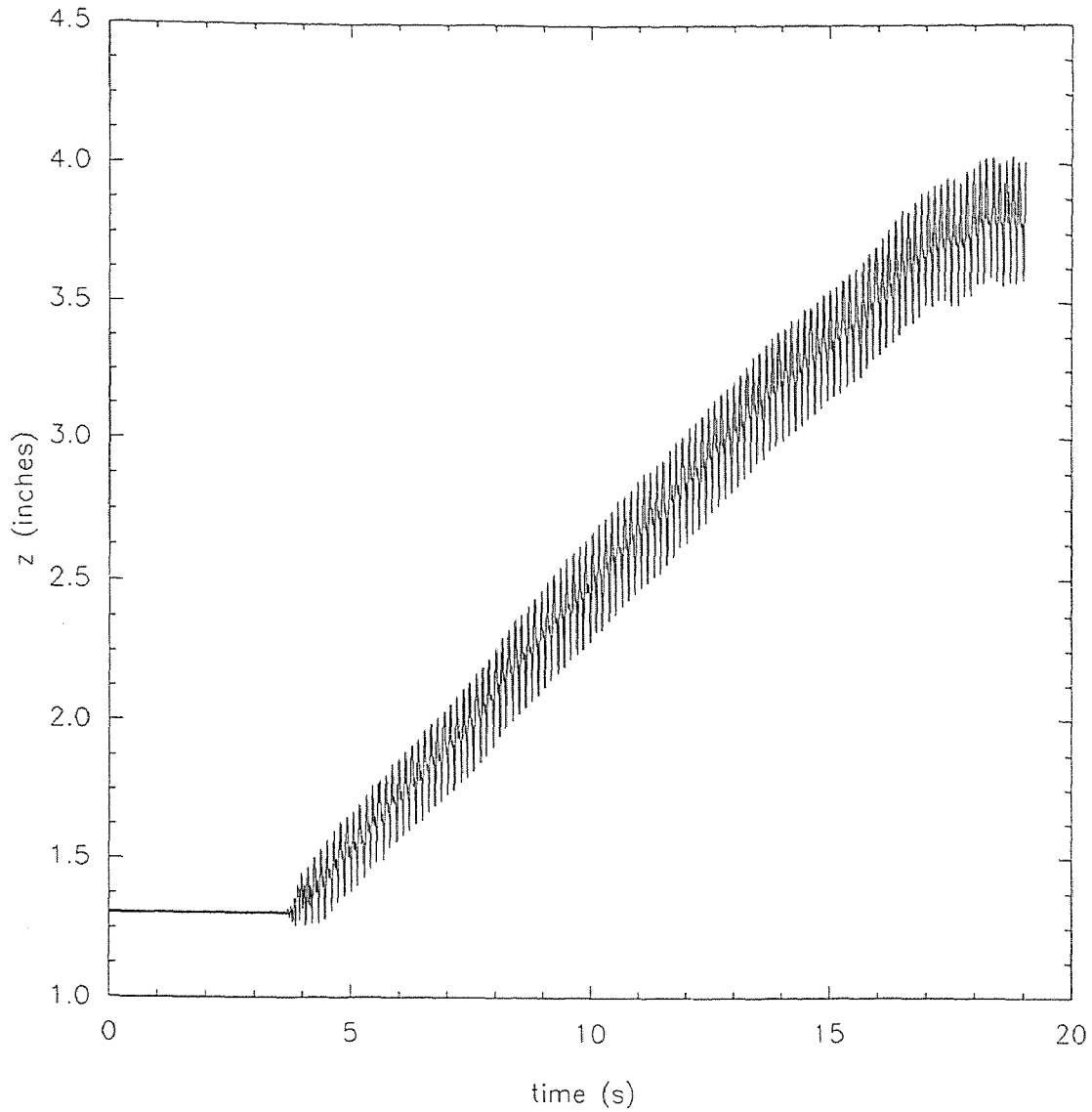


Figure 5.18 . Plot of the vertical position z as a function of time for $a/d = 1$ and $f = 15$ Hz. The ball is initially touching the side walls. The rise is linear with time, and the ball oscillates at $f/2$. No major differences with Fig. 5.12 are observed.

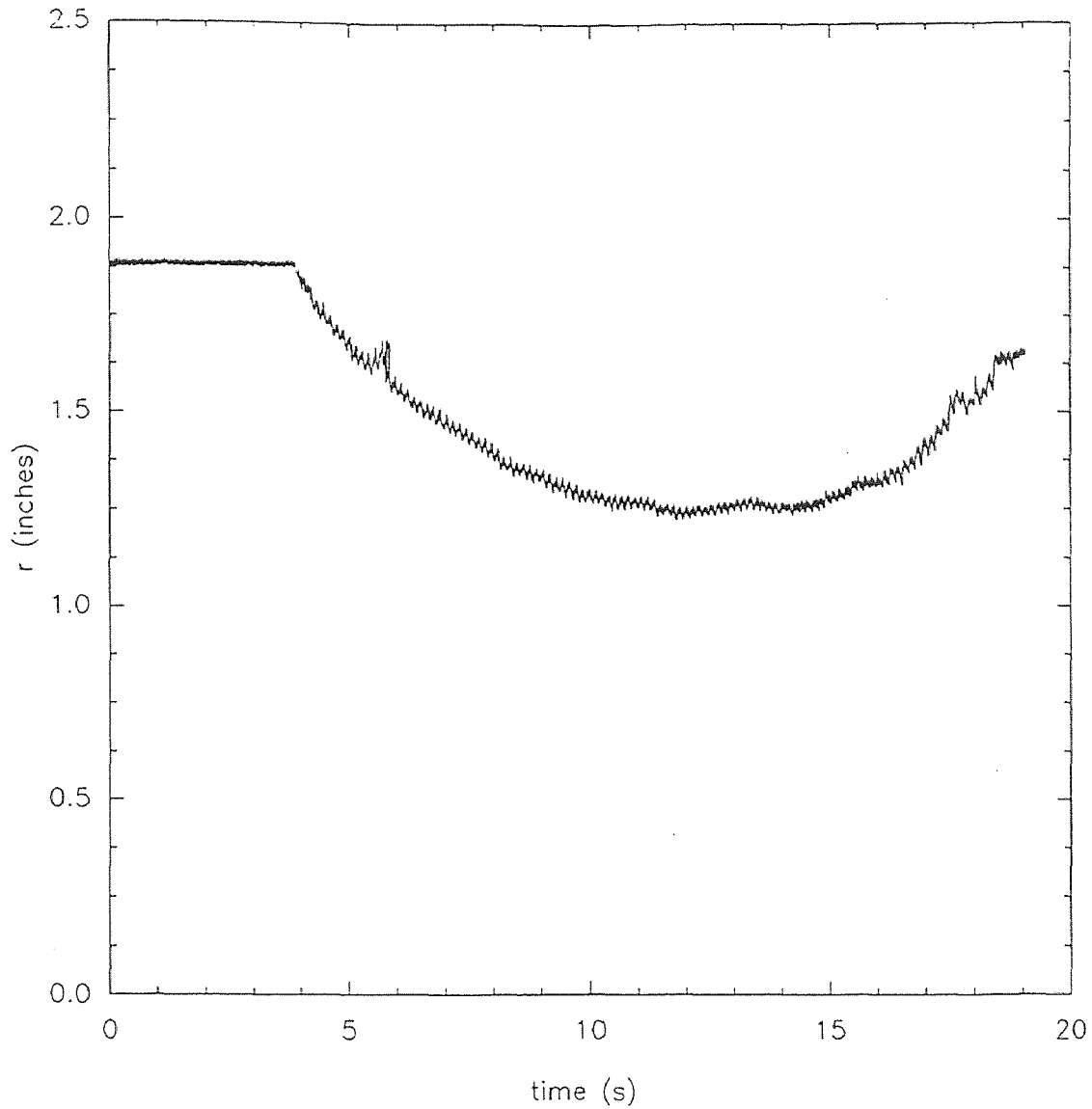


Figure 5.19. Plot of the radial displacement r as a function of time, for $a/d = 1$ and $f = 15$ Hz. First, the ball is observed to move from the walls towards the center of the cylinder. Before reaching the bed surface, the ball starts to move back towards the walls, apparently following the bulk convective flow.

the width of the downward flow ($3d$) observed on the bed surface. One could think the width of the downward flow can actually be $5d$ in some place. However, there must have an horizontal flow to allow the circulation of mass from the downward to the upward flow, and most probably, this horizontal flow is carrying the ball farther away from the walls than $3d$.

5.3 Problems and Possible Improvements

All the trajectories analysed by Fourier transform show a peak at high frequency, usually around 250 Hz. An example is given in Fig. 5.20. This peak can not be considered as noise, since the amplitude of noise usually decrease with frequency. The explanation for the existence of this peak certainly deserves to be found since it introduces unphysical fluctuations in the actual motion of the ball and affect the precision of the tracking technique.

Numerous computations of velocity and acceleration have been tested, and it appeared there was a huge sensibility to the noise. A time derivative in actual space results in a multiplication by frequency in Fourier space, and consequently the noise at high frequencies is amplified. To solve this problem smoothing techniques have been employed. One technique is the convolution of the trajectory by a Gaussian. The major disadvantage of this technique is the loss of energy in the signal. The suggested solution to this problem is to apply several times the Gaussian convolution to the difference between the original signal and the previously smoothed signal to gather some of the lost energy, but then a lot of details of the trajectory are lost. Another technique is to remove the high frequency noise in Fourier space, but then the sharpness of a collision may be lost.

The analysis of the trajectory itself is also a difficult task. For example, it is very difficult to obtain a phase “portrait”, i. e. the evolution of the ball position at a fixed vibration phase. This type of analysis is a major tool to understand the behavior of non-linear system. The main problem is that there is no reference between the trajectory and the motion of the piston. Consequently, a true time reference is missing, and the motion of the ball relative to the piston is unknown. If one want to find any kind of correlations in the motion of the ball from one period to the other, it is definitely important to include the

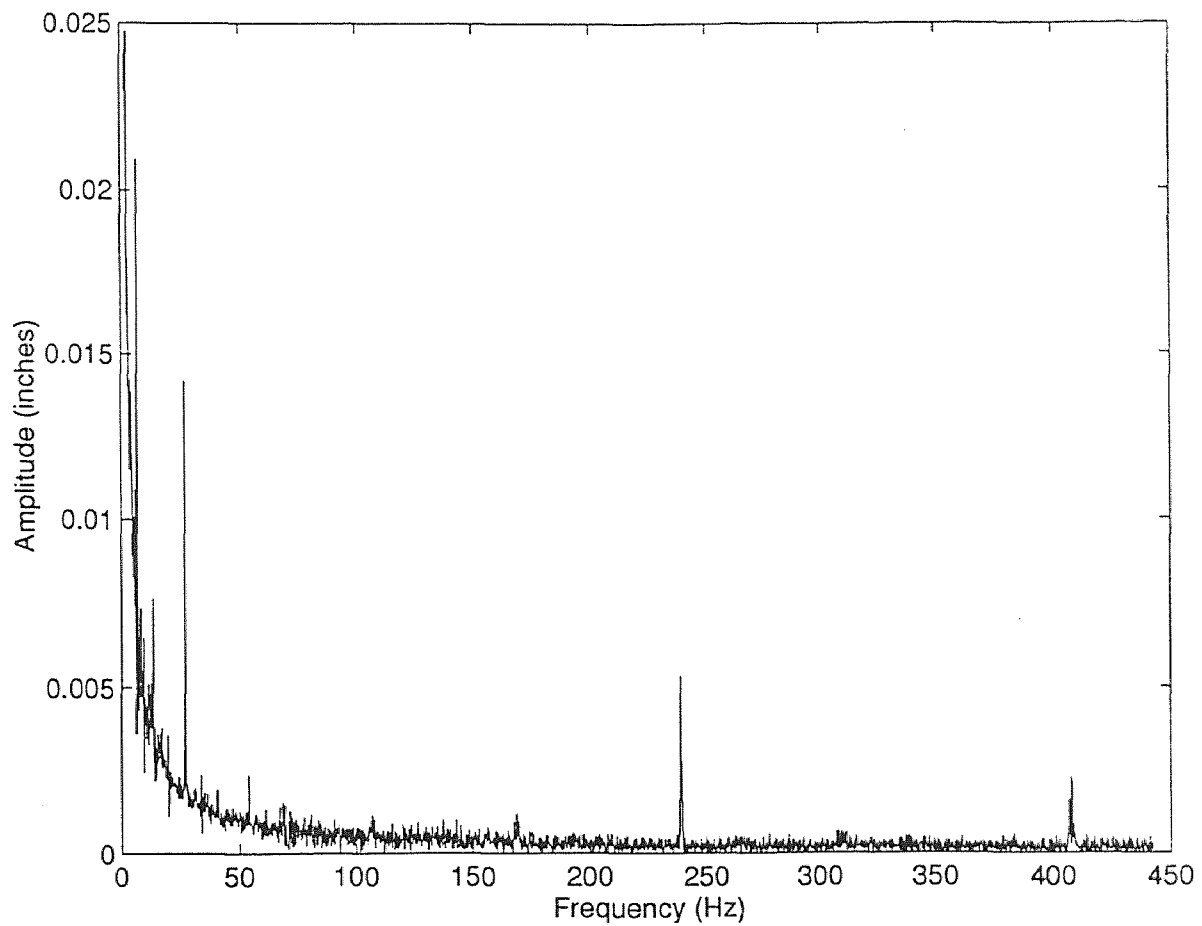


Figure 5.20. Amplitude spectrum corresponding to the trajectory of Fig. 5.5, when $a/d = 1.8$ and $f = 27$ Hz, showing at high frequency a peak around 250 Hz, whose origin is undetermined. Otherwise, there is three dominant peaks at f , $f/2$ and $f/4$, and there is a profile in $1/f$ corresponding to the FFT of the almost linear average motion.

motion of the piston in the acquisition procedure. For example, it could be a good idea to collect the signal coming from the accelerometer as a reference. To establish a phase “portrait”, it is also interesting to be able to fix the phase precisely. Since the acquisition rate of the data has nothing to do with the vibration frequency, the possibility to have a point at the same phase each period becomes fortuitous. Thus, it would be interesting to lock the acquisition on the vibration frequency with a variable waiting time between each data points. Each data points is constituted of 18 voltages readings which have to be read in a short period of time at the acquisition rate while the waiting time between the points can be much longer. With the actual acquisition board which possesses 16 channels, it is impossible to realize this goal because it requires to read in one sequence at least 18 channels.

A major problem is due to the tracking technique itself. The calibration procedures consist in taking the voltages induced when the ball is placed at the center of the cage and then rotated to obtain four different positions. Because the antennae cage used is small, there are important errors in the determination of the actual positions when the ball will be close to the antennae and not on a symmetry axis. One possible explanation is that the dipolar approximation is not valid anymore because the current loops (the transmitters) are too close to the antennae. Furthermore, one of the loops is very big in comparison to the others, and it is more difficult to fulfill the conditions for the dipolar approximation. It should be recalled that the magnetic field, created by the loop itself, may have some non negligible components in the loop plane. These components are clearly not taken in account in the model used for the determination of position from the induced voltages. The additional limitation for the study of segregation is that the amount of rising from one period to the other is often very small in comparison with the amplitude of the oscillatory motion of the ball. It means that the precision of the recorded trajectory must be extremely good to localize very tiny variations of the trajectory.

CHAPTER 6

CONCLUSION

The main conclusion is the existence of three rise regimes in which a single large sphere can rise to the surface of a vibrated bed of uniform particles. The first regime corresponds to the formation of heap, which coexists with convection, and the rise time is observed to increase exponentially with frequency when the relative acceleration is kept fixed. This first regime is observed for a frequency smaller than a critical frequency. In the second regime, the rise time is also increasing with frequency at fixed relative acceleration, but the variation is now dominated by an exponential of the square of frequency. Also, the large ball is carried upward by a convection flow where heaping is no more observed. Thus, a distinction must be made between a convective regime where heaping is observed, and a convective regime without heaping. In the third regime, the bed crystallizes and the rise time varies again exponentially with frequency. The third regime is called “non-convective” in the sense that the rise velocity depends on the size ratio. Because the particles are confined in a very stable crystal-like structure, it is likely that the rise phenomenon is controlled by structural defects due to the presence of the large ball (or intruder). Then, the more perturbed the structure, i. e. the larger the intruder, the faster is the rise.

The rise of a large sphere in a vibrated bed appears to be strongly dependent on the amplitude of vibration. For fixed relative accelerations, the smaller the amplitude, the longer the rise time. More important is the fact that a decrease in amplitude leads to the same relative increase of rise time whatever is the relative acceleration. In fact, the comparison with Ahmad’s experiments strongly suggests that a/d , the amplitude dimensioned by the diameter of the bed spheres, is the appropriate control parameter. Then, the rapid increase of rise time when the amplitude decreases can be understood as a finite size effect due to the discrete nature of the bed.

The observation of the trajectories reveals more on the dynamic of the rise. Trajectories have been described when there is heaping and where there is no heaping. No conclusive differences have been observed between the trajectories. An inverse convection

pattern has been observed when the bed undergoes a subharmonic bifurcation. It must be emphasized that this inverse convection is not simply a reversal of the usual convective pattern. A “whale” effect has been observed, but its physical nature is not understood. However, it is interesting that a single experimental configuration leads to the observation of so different behaviors. The analysis of the ball trajectory during the rise shows that no significant rotation of the ball occurs. Only two components of the motion are relevant : the vertical motion and the radial displacement. The radial displacement is nonexistent when the ball is situated at the center of the container, while it is maximum when the ball is positioned initially at the walls.

To date, more investigations need to be done. To be able to obtain more information from the trajectories, it is necessary to improve the tracking technique. The least is to simplify the data acquisition and make it more flexible so as to be able to measure physical parameters such as the motion of the ball at fixed phase. The experimental investigation of the rise time needs also more attention. The borders between the different regimes must be defined more precisely as a function of the vibration parameters, and their physical meaning needs to be understood. Recent observations of the piston acceleration have shown that the form of the vibration is not always sinusoidal as expected. In particular, the vibration is far from a sinusoid when the frequency is low. There is a non negligible possibility that the transition observed between the first and the second regime is an “artefact” due to the dependence of the vibration shape on the frequency. This last point absolutely needs to be clarified.

REFERENCES

- [1] S. B. Savage, and D. J. Jeffrey, "The stress tensor in a granular flow at high shear rates," *J. Fluid Mech.* **110**, 255 (1981).
- [2] C. K. K. Lun, S. B. Savage, D. J. Jeffrey, and N. Chepurnyi, "Kinetic theories for granular flow: inelastic particles in Couette flow and slightly inelastic particles in a general flowfield," *J. Fluid Mech.* **140**, 223 (1984).
- [3] J. T. Jenkins, and M. W. Richman, "Grad's 13-moment system for a dense gas of inelastic spheres," *Arch. Rat. Mech. Anal.* **87**, 355 (1985).
- [4] M. H. Cooke, D. J. Stephens and J. Bridgwater, "Powder mixing — A literature survey," *Powder Technology* **15**, 1 (1976).
- [5] L. T. Fan, and Yi-Ming Chen, "Recent developments in solids mixing," *Powder Technology* **61**, 255 (1990).
- [6] J. C. Williams, "The mixing of dry powders," *Powder Technology* **2**, 13 (1968).
- [7] S. B. Savage, "Flows of granular materials with applications to geophysical problems," IUTAM International Summer School on Mechanics, Udine, Italy (1992).
- [8] O. Reynolds, "On the dilatancy of media composed of rigid particles in contact," *Phil. Mag. S.* **20**, 469 (1885).
- [9] M. Faraday, *Phil. Trans. R. Soc. London* **52**, 299 (1831).
- [10] W. Kroll, *Chem. Ingr. Tech.* **27**, 33 (1955).
- [11] G. Rátkai, "Particle flow and mixing in vertically vibrated beds," *Powder Technology* **15**, 187 (1976).
- [12] S. Savage, "Streaming motions in a bed of vibrationally fluidized dry granular material," *J. Fluid Mech.* **194**, 457 (1988).
- [13] P. Evesque, and J. Rajchenbach, "Instability in a sand heap," *Phys. Rev. Lett.* **62**, 44 (1989).
- [14] C. Laroche, S. Douady, and S. Fauve, "Convective flow of granular masses under vertical vibrations," *J. Phys. France* **50**, 699 (1989).
- [15] H. K. Pak, E. Van Doorm, and R. P. Behringer, "Effects of ambient gases on granular materials under vertical vibration," *Phys. Rev. Lett.* **74**, 4643 (1995).

REFERENCES
(Continued)

- [16] E. Clement, J. Duran, and J. Rajchenbach, "Experimental study of heaping in a two-dimensional "sandpile"," *Phys. Rev. Lett.* **69**, 1189 (1992).
- [17] J. Rajchenbach, "Dilatant process for convection motion in a sand heap," *Europhys. Lett.* **16** (2), 149 (1991).
- [18] J. B. Knight, H. M. Jaeger, and S. R. Nagel, "Vibration-induced size separation in granular media: The convection connection," *Phys. Rev. Lett.* **70**, 3728 (1993).
- [19] J. B. Knight, E. E. Ehrichs, V. Yu. Kuperman, J. K. Flint, H. M. Jaeger, and S. R. Nagel, "An experimental study of granular convection," *Phys. Rev. E* **54**, 5726 (1996).
- [20] P. K. Haff, "Grain flow as a fluid-mechanical phenomenon," *J. Fluid Mech.* **134**, 401 (1983).
- [21] P. Evesque, E. Szmatala, and J. P. Denis, "Surface fluidization of a sand pile," *Europhys. Lett.* **12** (7), 623 (1990).
- [22] E. Clement, and J. Rajchenbach, "Fluidization of a bidimensional powder," *Europhys. Lett.* **16** (2), 133 (1991).
- [23] S. Warr, J. M. Huntley, and G. T. H. Jacques, "Fluidization of a two-dimensional granular system: Experimental study and scaling behavior," *Phys. Rev. E* **52**, 5583 (1995).
- [24] S. Douady, S. Fauve, and C. Laroche, "Subharmonic instabilities and defects in a granular layer under vertical vibrations," *Europhys. Lett.* **8** (7), 621 (1989).
- [25] H. K. Pak, and R. P. Behringer, "Surface waves in vertically vibrated granular materials," *Phys. Rev. Lett.* **71**, 1832 (1993).
- [26] E. Clement, L. Vanel, J. Rajchenbach, and J. Duran, "Pattern formation in a vibrated granular layer," *Phys. Rev. E* **53**, 2972 (1996).
- [27] F. Melo, P. B. Umbanhowar, and H. L. Swinney, "Hexagons, kinks and disorder in oscillated granular layers," *Phys. Rev. Lett.* **75**, 3838 (1995).
- [28] W. S. Edwards, and S. Fauve, "Patterns and quasi-patterns in the Faraday experiment," *J. Fluid Mech.* **27** 123 (1994).

REFERENCES
(Continued)

- [29] T. H. Metcalf, J. B. Knight, and H. M. Jaeger, "Standing wave patterns in shallow beds of vibrated granular material," preprint.
- [30] H. E. White, and S. F. Walton, "Particle packing and particle shape," *J. Am. Ceram. Soc.* **20**, 155 (1937).
- [31] M. Leva, and M. Grummer, "Pressure drop through packed tubes: III, Prediction of voids in packed tubes," *Chem. Eng. Prog.* **43**, 713 (1947).
- [32] A. E. R. Westman, and H. R. Hugill, "Packing of particles," *J. Am. Ceram. Soc.* **13**, 767 (1930).
- [33] J. E. Ayer, and F. E. Soppet, "Vibratory compaction: I, Compaction of spherical shapes," *J. Am. Ceram. Soc.* **48**, 180 (1965).
- [34] T. G. Owe Berg, R. L. McDonald, and R. J. Trainor, Jr, "The packing of spheres," *Powder Technology* **3**, 183 (1969).
- [35] J. B. Knight, C. G. Fandrich, C. N. Lau, H. M. Jaeger, and S. R. Nagel, "Density relaxation in a vibrated granular material," *Phys. Rev. E* **51**, 3957 (1995).
- [36] G. C. Barker, and A. Mehta, "Transient phenomena, self-diffusion, and orientational effects in vibrated powders," *Phys. Rev. E* **47**, 184 (1993).
- [37] C. A. G. Weymouth, "Effect of particle interference in mortars and concret," *Rock. Prod.* **36** (2), 26 (1933).
- [38] R. L Brown, "The fundamental principles of segregation," *J. Inst. Fuel* **13**, 15 (1939).
- [39] J. L. Olsen, and E. G. Rippie, "Segregation kinetics of particulate solids systems: I, Influence of particle size and particle size distribution," *J. Pharm. Sci.* **53**, 147 (1964).
- [40] E. G. Rippie, J. L. Olsen, and M. D. Faiman, "Segregation kinetics of particulate solids systems: II, Particle density-size interactions and wall effects," *J. Pharm. Sci.* **53**, 1360 (1964).
- [41] M. D. Faiman, and E. G. Rippie, "Segregation kinetics of particulate solids systems: III, Dependence on agitation intensity," *J. Pharm. Sci.* **54**, 719 (1965).

REFERENCES
(Continued)

- [42] J. C. Williams, "Segregation of powders and granular materials," *Fuel Soc. J. (Univ. of Sheffield)* **14**, 29 (1963).
- [43] K. Ahmad, and I. J. Smalley, "Observation of a particle segregation in vibrated granular systems," *Powder Technology* **8**, 69 (1973).
- [44] J. Duran, T. Maozi, E. Clement, and J. Rajchenbach, "Size segregation in a two-dimensional sandpile: Convection and arching effects," *Phys. Rev. E* **50**, 5138 (1994).
- [45] J. Duran, J. Rajchenbach, and E. Clement, "Arching effect model for particle size segregation," *Phys. Rev. Lett.* **70**, 2431 (1993).
- [46] W. Cooke, S. Warr, J. M. Huntley, and R. C. Ball, "Particle size segregation in a two-dimensional bed undergoing vertical vibration," *Phys. Rev. E* **53**, 2812 (1996).
- [47] P. K. Haff, and B. T. Werner, "Computer simulation of the mechanical sorting of grains," *Powder Technology* **48**, 239 (1986).
- [48] A. Rosato, F. Prinz, K. J. Strandburg, and R. H. Swendsen, "Monte-Carlo simulation of particulate matter segregation," *Powder Technology* **49**, 59 (1986).
- [49] A. Rosato, K. J. Strandburg, F. Prinz, and R. H. Swendsen, "Why the Brazil nuts are on top: Segregation of particulate matter by shaking," *Phys. Rev. Lett.* **58**, 1038 (1987).
- [50] R. Jullien, P. Meakin, and A. Pavlovitch, "Three-dimensional model for particle size-segregation by shaking," *Phys. Rev. Lett.* **69**, 640 (1992).
- [51] R. Jullien, and P. Meakin, "A mechanism for particle size-segregation in three dimensions," *Nature* **334**, 425 (1990).
- [52] R. Jullien, and P. Meakin, "Particle size-segregation by shaking in two-dimensional disk packings," *Europhys. Lett.* **22** (7), 523 (1993).
- [53] S. Dippel, and S. Luding, "Simulations on size-segregation: Geometrical effects in the absence of convection," *J. Phys. I France* **5**, 1527 (1995).
- [54] G. C. Barker, A. Mehta, and M. J. Grimson, "Comment on "Three-dimensional model for particle size segregation by shaking." by R. Jullien et al," *Phys. Rev. Lett.* **70**, 2194 (1993).

REFERENCES (Continued)

- [55] A. Mehta, and G. C. Barker, "Vibrated powders: A microscopic approach," *Phys. Rev. Lett.* **67**, 394 (1991).
- [56] G. C. Barker, and A. Mehta, "Transient phenomena, self-diffusion, and orientational effects in vibrated powders," *Phys. Rev. E* **47**, 184 (1993).
- [57] G. C. Barker, and A. Mehta, "Comment on "Particle size segregation by shaking in two-dimensional disk packings" by R.Jullien et al," *Europhys. Lett.* **29** (1), 61 (1995).
- [58] T. Ohtsuki, D. Kinoshita, Y. Takemoto, and A. Hayashi, "Segregation by shaking in cohesionless granular mixtures: Effects of particle size and density," *J. of Phys. Soc. of Japan* **64**, 430 (1995).
- [59] Y-h. Taguchi, "New origin of a convective motion: Elastically induced convection in granular materials," *Phys. Rev. Lett.* **69**, 1367 (1992).
- [60] J. A. C. Gallas, H. J. Herrmann, and S. Sokolowski, "Convection cells in vibrating granular media," *Phys. Rev. Lett.* **69**, 1371 (1992).
- [61] T. Pöschel, and H. J. Herrmann, "Size segregation and convection," *Europhys. Lett.* **29** (2), 123 (1995).
- [62] J. A. C. Gallas, H. J. Herrmann, T. Pöschel, and S. Sokolowski, "Molecular dynamics of size segregation in three dimensions," *J. Stat. Phys.* **82**, 443 (1996).
- [63] Y. Lan, and A. D. Rosato, "Convection related phenomenon in granular dynamics simulations of vibrated beds," preprint.
- [64] G. C. Barker, and A. Mehta, "Size segregation mechanisms," *Nature* **364**, 5 august 1993.
- [65] R. N. Dave, and B. G. Bukiet, "Non-intrusive rigid body tracking technique for dry particulate flows, Part I: Theoretical aspects," submitted to Measurement Science and Technology (Formerly Physics E), 1994.
- [66] J. R. Volcy, "Development of a non-intrusive particle motion tracking technique for granular flow experiments," *MS thesis*, New Jersey Institute of Technology, Newark, New Jersey, 1994.

REFERENCES
(Continued)

- [67] P. B. Patel, "Simulation study of the particle tracking system," *MS Thesis*, Department of Mechanical Engineering, New Jersey Institute of Technology, Newark, New Jersey, 1995.
- [68] V. B. Gupta, "Implementation of a three-dimensional non-intrusive particle tracking technique," *MS Thesis*, Department of Mechanical Engineering, New Jersey Institute of Technology, Newark, New Jersey, 1995.
- [69] M. C. Cross, and P. C. Hohenberg, "Pattern formation outside of equilibrium," *Rev. Mod. Phys.* **65**, 851 (1993).